Single chargino production at linear colliders

G. Moreau
Service de Physique Théorique
CE-Saclay F-91191 Gif-sur-Yvette, Cedex France

September 12, 2000

LC-TH-2000-040

Abstract

We study the single chargino production $e^+e^- \to \tilde{\chi}^{\pm}\mu^{\mp}$ at linear colliders which occurs through the λ_{121} R-parity violating coupling constant. We focus on the final state containing 4 leptons and some missing energy. The largest background is supersymmetric and can be reduced using the initial beam polarization and some cuts based on the specific kinematics of the single chargino production. Assuming the highest allowed supersymmetric background, a center of mass energy of $\sqrt{s} = 500GeV$ and a luminosity of $\mathcal{L} = 500fb^{-1}$, the sensitivities on the λ_{121} coupling constant obtained from the single chargino production study improve the low-energy experimental limit over a range of $\Delta m_{\tilde{\nu}} \approx 500GeV$ around the sneutrino resonance, and reach values of $\sim 10^{-4}$ at the $\tilde{\nu}$ pole. The single chargino production also allows to reconstruct the $\tilde{\chi}_1^{\pm}$, $\tilde{\chi}_2^{\pm}$ and $\tilde{\nu}$ masses. The initial state radiation plays a fundamental role in this study.

1 Introduction

In supersymmetric theories, there is no clear theoretical argument in favor of the conservation of the so-called R-parity symmetry, either from the point of view of grand unified models, string theories or scenarios with discrete gauge symmetries [1]. The phenomenology of supersymmetry (SUSY) at futur colliders would change fundamentally if the R-parity symmetry were violated. Indeed, in such a scenario the typical missing energy signature caused by the stable nature of the Lightest Supersymmetric Particle (LSP) would be replaced by multijet or multileptonic signals, depending on what are the dominant R-parity violating ($\not{R}_p$) couplings. The reason is that the $\not{R}_p$ terms of the superpotential trilinear in the quarks and leptons superfields (see Eq.(1)) allow the LSP, whatever it is, to decay.

$$W_{\not{R}_p} = \sum_{i,j,k} \left(\frac{1}{2}\lambda_{ijk} L_i L_j E_k^c + \lambda'_{ijk} L_i Q_j D_k^c + \frac{1}{2}\lambda''_{ijk} U_i^c D_j^c D_k^c \right). \quad (1)$$

The effects of the $\not{R}_p$ decays of the LSP on the study of SUSY particles pair production have been considered in the context of linear colliders [2] and futur hadronic colliders, namely the Tevatron (Run II) [3, 4, 5, 6] and the LHC [7].

The measure of the $\not{R}_p$ coupling constants of Eq.(1) could be performed via the detection of the displaced vertex associated to the decay of the LSP. The sensitivities on the $\not{R}_p$ couplings obtained through this method depend on the detector geometry and performances. Let us estimate the largest values of the $\not{R}_p$ coupling constants that can be measured via the displaced vertex analysis. We suppose that the LSP is the lightest neutralino ($\tilde{\chi}_1^0$). The flight length of the LSP in the laboratory frame is then given in meters by [8],

$$c\gamma\tau \sim 3\gamma\ 10^{-3} m (\frac{\tilde{m}}{100GeV})^4 (\frac{1GeV}{m_{LSP}})^5 (\frac{1}{\Lambda})^2, \quad (2)$$

where $\Lambda = \lambda$, λ' or λ'', c is the light speed, γ the Lorentz boost factor, τ the LSP life time, m_{LSP} the LSP mass and $\tilde{m}$ the mass of the supersymmetric scalar particle involved in the three-body decay of the LSP.

Since the displaced vertex analysis is an experimental challenge at hadronic colliders, we consider here the linear colliders. Assuming that the minimum distance between two vertex necessary to distinguish them experimentally is of order $2\ 10^{-5}m$ at linear colliders, we see from Eq.(2) that the $\not{R}_p$ couplings could be measured up to the values,

$$\Lambda < 1.2\ 10^{-4}\gamma^{1/2}(\frac{\tilde{m}}{100GeV})^2(\frac{100GeV}{m_{LSP}})^{5/2}. \tag{3}$$

There is a gap between these values and the low-energy experimental constraints on the $\not{R}_p$ couplings which range typically in the interval $\Lambda < 10^{-1} - 10^{-2}$ for superpartners masses of $100GeV$ [1, 9, 10]. However, the domain lying between these low-energy bounds and the values of Eq.(3) can be tested through another way: The study of the production of either Standard Model or SUSY particles involving $\not{R}_p$ couplings. Indeed, the cross sections of such productions are directly proportional to a power of the relevant $\not{R}_p$ coupling constant(s), which allows to determine the values of the $\not{R}_p$ couplings. Therefore, there exists a complementarity between the displaced vertex analysis and the study of reactions involving $\not{R}_p$ couplings, since these two methods allow to investigate different ranges of values of the $\not{R}_p$ coupling constants.

The studies of the $\not{R}_p$ contributions to Standard Model particle productions have been performed both at leptonic [11]-[28] and hadronic [29]-[35] colliders. Those contributions generally involve two $\not{R}_p$ vertex and have thus some rates proportional to Λ^4. The processes involving only one $\not{R}_p$ vertex are less suppressed since the $\not{R}_p$ couplings incur stringent experimental limits [1, 9, 10]. Those reactions correspond to the single production of supersymmetric particle. Another interest of the single superpartner production is the possibility to produce SUSY particles at lower energies than through the superpartner pair production, which is the favored reaction in R-parity conserved models.

At hadronic colliders, the single superpartner production involves either λ' or λ'' coupling constants [8, 29, 36, 37, 38, 39, 40, 41]. The test of the λ couplings via the single superpartner production can only be performed at leptonic colliders. At leptonic colliders, either gaugino (not including gluino) [12, 42, 43, 44] or slepton (charged or neutral) [44] can be singly produced in the simple $e^+e^- \to 2-body$ reactions. The single production of slepton has a reduced phase space, since the slepton is produced together with a Z or W gauge boson. In contrast, the $\tilde{\chi}_1^0$ is produced together with a neutrino. Nevertheless, if the $\tilde{\chi}_1^0$ is the LSP, as in many supersymmetric scenarios, it undergoes an $\not{R}_p$ decay which reads as $\tilde{\chi}_1^0 \to l\bar{l}\nu$ if one assumes a dominant λ Yukawa coupling. Therefore, the single $\tilde{\chi}_1^0$ production leads typically to the $2l + \not{E}$ final state which has a large Standard Model background. In this paper, we focus on the single chargino production $e^+e^- \to \tilde{\chi}^{\pm}l_m^{\mp}$, which occurs through the $\not{R}_p$ coupling constants λ_{1m1} ($m = 2$ or 3). There are several motivations. First, the single chargino production has an higher cross section than the single neutralino production [44]. Moreover, it can lead to particularly interesting multileptonic signatures due to the cascade decay initiated by the chargino.

The single gaugino productions at e^+e^- colliders have t and u channels and can also receive a contribution from the resonant sneutrino production. At $\sqrt{s} = 200GeV$, the off-resonance rates of the single chargino and neutralino productions are typically of order $100fb$ and $10fb$, respectively [44], for a value of the relevant $\not{R}_p$ coupling constant equal to its low-enery bound for $m_{\tilde{e}_R} = 100GeV$: $\lambda_{1m1} = 0.05$ [9]. The off-pole effects of the single gaugino production are thus at the limit of observability at LEP II assuming an integrated luminosity of $\mathcal{L} \approx 200pb^{-1}$. At the sneutrino resonance, the single gaugino production has higher cross section values. For instance with $\lambda_{1m1} = 0.01$, the chargino production rate can reach $2\ 10^{-1}pb$ at the resonance [42]. This is the reason why the experimental analysis of the single gaugino production at the LEP collider [20, 21, 22, 23, 24] allows to test $\not{R}_p$ couplings values smaller than the low-energy bounds only at the sneutrino resonance $\sqrt{s} = m_{\tilde{\nu}}$ and, due to the Initial State Radiation (ISR) effect, in a range of typically $\sim 50GeV$ around the $\tilde{\nu}$ pole. The sensitivities on the λ_{1m1} couplings obtained at LEP reach values of order 10^{-3} at the sneutrino resonance.

The experimental analysis of the single gaugino production at futur linear colliders should be interesting due to the high luminosities and energies expected at these futur colliders [45, 46]. However, the single gaugino production might suffer a large SUSY background at linear colliders. Indeed, due to the high energies reached at these colliders, the pair productions of SUSY particles may have important cross sections.

In this article, we study the single chargino production via the λ_{121} coupling at linear colliders and we consider the final state containing 4 leptons plus some missing energy ($\not{E}$). We show that the SUSY background can be greatly reduced with respect to the signal. This discrimination is based on the two

following points: First, the SUSY background can be suppressed by making use of the beam polarization capability of the linear colliders. Secondly, the specific kinematics of the single chargino production reaction allows to put some efficient cuts on the transverse momentum of the lepton produced together with the chargino. We find that, by consequence of this background reduction, the sensitivity on the λ_{121} coupling obtained at the $\tilde{\nu}$ resonance at linear colliders for $\sqrt{s} = 500GeV$ and $\mathcal{L} = 500fb^{-1}$ [45] would be of order 10^{-4}, namely one order of magnitude better than the results of the LEP analysis [20, 21, 22, 23, 24], assuming the largest supersymmetric background allowed by the experimental limits on the SUSY masses.

Besides, in the scenario of a single dominant $\not{R}_p$ coupling of type λ with $\tilde{\chi}_1^0$ as the LSP, the experimental superpartner mass reconstruction from the SUSY particle pair production suffers an high combinatorial background both at linear colliders [2] and LHC [7]. The reason is that all the masses reconstructions are based on the $\tilde{\chi}_1^0$ reconstruction which is degraded by the imperfect identification of the charged leptons generated in the decays of the 2 neutralinos as $\tilde{\chi}_1^0 \to l\bar{l}\nu$, and the presence of missing energy in the final state. In particular, the chargino mass reconstruction in the leptonic channel is difficult since the presence of an additional neutrino, coming from the decay $\tilde{\chi}^{\pm} \to \tilde{\chi}^0 l\nu$, renders the control on the missing energy more challenging. In this paper, we show that through the study of the $4l + \not{E}$ final state, the specific kinematics of the single chargino production reaction at linear colliders allows to determine the $\tilde{\chi}_{1,2}^{\pm}$ and $\tilde{\nu}$ masses.

In Section 2 we define the theoretical framework. In Sections 3 and 4 we describe the signal and the several backgrounds. In Section 5, we present the sensitivity on the SUSY parameters that can be obtained in an e^+e^- machine allowing an initial beam polarization. In this last section, we also show how some information on the SUSY mass spectrum can be derived from the study of the single chargino production, and we comment on another kind of signature: the $3l + 2jets + \not{E}$ final state.

2 Theoretical framework

We work within the Minimal Supersymmetric Standard Model (MSSM) which has the minimal particle content and the minimal gauge group $SU(3)_C \times SU(2)_L \times U(1)_Y$, namely the Standard Model gauge symmetry. The supersymmetric parameters defined at the electroweak scale are the Higgsino mixing parameter μ, the ratio of the vacuum expectation values of the two Higgs doublet fields $\tan\beta =< H_u > / < H_d >$ and the soft SUSY breaking parameters, namely the bino ($\tilde{B}$) mass M_1, the wino ($\tilde{W}$) mass M_2, the gluino ($\tilde{g}$) mass M_3, the sfermion masses $m_{\tilde{f}}$ and the trilinear Yukawa couplings A. The remaining three parameters $m_{H_u}^2$, $m_{H_d}^2$ and the soft SUSY breaking bilinear coupling B are determined through the electroweak symmetry breaking conditions, which are two necessary minimization conditions of the Higgs potential.

We assume that all phases in the soft SUSY breaking potential are equal to zero in order to eliminate all new sources of CP violation which are constrained by extremely tight experimental limits on the electron and neutron electric moments. Furthermore, to avoid any problem of Flavor Changing Neutral Currents, we take the matrices in flavor space of the sfermion masses and A couplings close to the unit matrix. In particular, for simplification reason we consider vanishing A couplings. This last assumption concerns the splitting between the Left and Right sfermions masses and does not affect our analysis which depends mainly on the relative values of the sleptons, squarks and gauginos masses as we will discuss in next sections.

Besides, we suppose the R-parity symmetry to be violated so that the interactions written in the superpotential of Eq.(1) are present. The existence of a hierarchy among the values of the $\not{R}_p$ couplings is suggested by the analogy of those couplings with the Yukawa couplings. We thus assume a single dominant $\not{R}_p$ coupling of the type λ_{1m1} which allows the single chargino production at e^+e^- colliders.

Finally, we choose the LSP to be the $\tilde{\chi}_1^0$ neutralino since it is often real in many models, such as the supergravity inspired models.

3 Signal

The single chargino production $e^+e^- \to \tilde{\chi}^{\pm} l_m^{\mp}$ occurs via the λ_{1m1} coupling constant either through the exchange of a $\tilde{\nu}_{mL}$ sneutrino in the s channel or a $\tilde{\nu}_{eL}$ sneutrino in the t channel (see Fig.1). Due to the antisymmetry of the λ_{ijk} Yukawa couplings in the i and j indices, only a muon or a tau-lepton can be

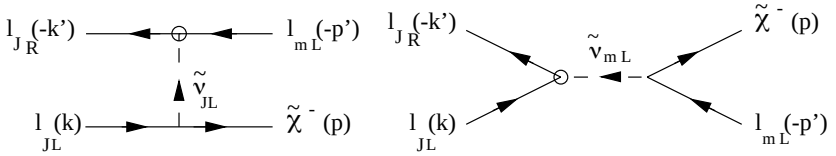

Figure 1: *Feynman diagrams of the single chargino production process at leptonic colliders. The $R\!\!\!/_p$ coupling constant λ_{JmJ} ($J = 1$, $m = 2$ or 3 for e^+e^- colliders and $J = 2$, $m = 1$ or 3 for $\mu^+\mu^-$ colliders) is symbolised by a small circle, and the arrows denote the flow of momentum of the corresponding particles. The Left and Right helicities of the particles are denoted by L and R, respectively, and the momentum of the particles by k,k',p and p'. The higgsino contribution as well as the charge conjugated process are not represented.*

produced together with the chargino, namely $m = 2$ or 3. The produced chargino can decay into the LSP as $\tilde{\chi}^{\pm} \to \tilde{\chi}^0_1 l\nu$ or as $\tilde{\chi}^{\pm} \to \tilde{\chi}^0_1 ud$. Then the LSP decays as $\tilde{\chi}^0_1 \to \bar{e}e\nu_m$, $\bar{e}e\bar{\nu}_m$, $l_m\bar{e}\bar{\nu}_e$ or $\bar{l}_m e\nu_e$ through λ_{1m1}. Each of these 4 $\tilde{\chi}^0_1$ decay channels has a branching ratio exactly equal to 25%. In this paper, we study the $4l + \not{E}$ final state generated by the decay $\tilde{\chi}^{\pm} \to \tilde{\chi}^0_1 l\nu$ of the produced chargino.

The single chargino production has a specific feature which is particularly attractive: Because of the simple kinematics of $2 \to 2 - body$ type reaction, the energy of the lepton produced with the chargino, which we write $E(l_m)$, is completely fixed by the center of mass energy $\sqrt{s}$, the lepton mass m_{l_m} and the chargino mass $m_{\tilde{\chi}^{\pm}}$:

$$E(l_m) = \frac{s + m^2_{l_m} - m^2_{\tilde{\chi}^{\pm}}}{2\sqrt{s}}. \tag{4}$$

The lepton momentum $P(l_m)$, which is related to the lepton energy by $P(l_m) = (E(l_m)^2 - m^2_{l_m} c^4)^{1/2}/c$, is thus also fixed. Therefore, the momentum distribution of the produced lepton is peaked and offers the opportunity to put some cuts allowing an effective discrimination between the signal and the several backgrounds. Besides, the momentum value of the produced lepton gives the $\tilde{\chi}^{\pm}$ mass through Eq.(4). Nevertheless, for a significant ISR effect the radiated photon carries a non negligible energy and the single chargino production must be treated as a three-body reaction of the type $e^+e^- \to \tilde{\chi}^{\pm} l^{\mp}_m \gamma$. Therefore, the energy of the produced lepton is not fixed anymore by the SUSY parameters. As we will show in Section 5.3.2, in this situation the transverse momentum of the produced lepton is more appropriate to apply some cuts and reconstruct the $\tilde{\chi}^{\pm}$ mass.
In the case where the produced lepton is a tau, the momentum of the lepton ($e^{\pm}$ or $\mu^{\pm}$) coming from the τ-decay is of course not peaked at a given value. Moreover, in contrast with the muon momentum, the precise determination of the tau-lepton momentum is difficult experimentally due to the unstable nature of the τ. From this point of view, the case of a single dominant λ_{121} coupling constant is a more promising scenario than the situation in which λ_{131} is the dominant coupling. Hence, from now on we focus on the single dominant $R\!\!\!/_p$ coupling λ_{121} and consider the single chargino production $e^+e^- \to \tilde{\chi}^{\pm}\mu^{\mp}$.

At this stage, an important remark can be made concerning the initial state. As can be seen from Fig.1, in the single $\tilde{\chi}^-$ production the initial electron and positron have the same helicity, namely, they are both Left-handed. Similarly in the $\tilde{\chi}^+$ production, the electron and the positron are both Right-handed. The incoming lepton and anti-lepton have thus in any case the same helicity. This is due to the particular structure of the trilinear $R\!\!\!/_p$ couplings which flips the chirality of the fermion. The incoming electron and positron could also have identical helicities. However, this contribution involves the higgsino component of the chargino and is thus suppressed by the coupling of the higgsino to leptons which is proportional to $m_l/(m_W \cos\beta)$. This same helicity property, which is characteristic of all type of single superpartner production at leptonic colliders [44], allows to increase the single chargino production rate by selecting same helicities initial leptons.

4 Background

4.1 Non-physic background

First, one has to consider the non-physic background for the $4l + \not{E}$ signature. The main source of such a background is the Z-boson pair production with ISR. Indeed, the ISR photons have an high probability to be colinear to the beam axis. They will thus often be missed experimentally becoming then a source of missing energy. The four leptons can come from the leptonic decays of the 2 Z-bosons. This background can be greatly reduced by excluding the same flavor opposite-sign dileptons which have an invariant mass in the range, $10GeV < |M_{inv}(l_p\bar{l}_p) - M_Z|$, $p = 1, 2, 3$ being the generation indice. Furthermore, the missing energy coming from the ISR is mainly present at small angles with respect to the beam axis. This point can be exploited to perform a better selection of the signal. As a matter of fact, the missing energy coming from the signal has a significant transverse component since it is caused by the presence of neutrinos in the final state. In Fig.2, we present the distribution of the transverse missing energy in the $4l + \not{E}$ events generated by the single $\tilde{\chi}_1^{\pm}$ production for a sneutrino mass of $m_{\tilde{\nu}} = 240GeV$ and for the point A of the SUSY parameter space defined as: $M_1 = 200GeV$, $M_2 = 250GeV$, $\mu = 150GeV$, $\tan\beta = 3$, $m_{\tilde{l}^{\pm}} = 300GeV$ and $m_{\tilde{q}} = 600GeV$ ($m_{\tilde{\chi}_1^{\pm}} = 115.7GeV$, $m_{\tilde{\chi}_1^0} = 101.9GeV$, $m_{\tilde{\chi}_2^0} = 154.5GeV$). The cut on the lepton momentum mentioned in Section 3 can also enhance the signal-to-background ratio. Finally, the beam polarization may be useful in reducing this source of background. Indeed, the initial leptons in the ZZ production process have opposite helicities. The reason is that the $Z - f - \bar{f}$ vertex conserves the fermion chirality. Furthermore, recall that in our signal, the initial electron and positron have similar helicities. Thus if the beam polarization at linear collider were chosen in order to favor opposite helicities initial states, the signal would be enhanced while the ZZ background would be suppressed. Since the polarization expected at linear colliders is of order 85% for the electron and 60% for the positron [45], the ZZ background would not be entirely eliminated by the beam polarization effect.

4.2 Standard Model background

The Standard Model backgrounds for the $4l+\not{E}$ signal come from $2 \to 3-body$ processes. For example, the $e^+e^- \to Z^0Z^0Z^0$ reaction can give rise to the four leptons plus missing energy signature. Another source of Standard Model background is the $e^+e^- \to Z^0W^+W^-$ reaction. The rates for those backgrounds have been calculated in [2] after the cuts on the charged lepton rapidity, $|\eta(l)| < 3$, the charged lepton transverse momentum, $P_t(l) > 10GeV$, and the missing transverse energy, $\not{E}_t > 20GeV$, have been applied. The results are the followings. The ZZZ production cross section does not exceed $1fb$. The ZWW production has a cross section of $0.4fb$ ($0.1fb$) at $\sqrt{s} = 500GeV$ ($350GeV$) after convoluting with the branching fractions for the leptonic decays of the gauge bosons. This rate value is obtained without the ISR effect which should reduce the cross section of the ZWW production dominated by the t channel exchange contribution [2]. As before, the ZWW production can be reduced using simultaneously the cut on the lepton momentum indicated in Section 3, the dilepton invariant mass cut and the beam polarization effect. Indeed, the initial leptons have opposite helicities in both the s and t channels of the process $e^+e^- \to Z^0W^+W^-$, as in the ZZ production process.

4.3 Supersymmetric background

The main sources of supersymmetric background to the $4l+\not{E}$ signature are the neutralinos and sneutrinos pair productions.

First, the reaction,

$$e^+e^- \to \tilde{\chi}_1^0 + \tilde{\chi}_1^0, \tag{5}$$

represents a background for the $4l + \not{E}$ signature since the $\tilde{\chi}_1^0$, which is the LSP in our framework, decays as $\tilde{\chi}_1^0 \to \bar{e}e\nu_\mu$, $\bar{e}e\bar{\nu}_\mu$, $\mu\bar{e}\bar{\nu}_e$ or $\bar{\mu}e\nu_e$ through the λ_{121} coupling. Therefore, the $\tilde{\chi}_i^0\tilde{\chi}_j^0$ productions (where $i = 1, ..., 4$ and $j = 1, ..., 4$ are not equal to 1 simultaneously) leading through cascade decays to a pair of $\tilde{\chi}_1^0$ accompanied by some neutrinos give also rise to the final state with 4 leptons plus some missing energy. These reactions are the following,

$$e^+e^- \to \tilde{\chi}_i^0 + \tilde{\chi}_1^0 \to \tilde{\chi}_1^0\nu_p\bar{\nu}_p + \tilde{\chi}_1^0, \tag{6}$$

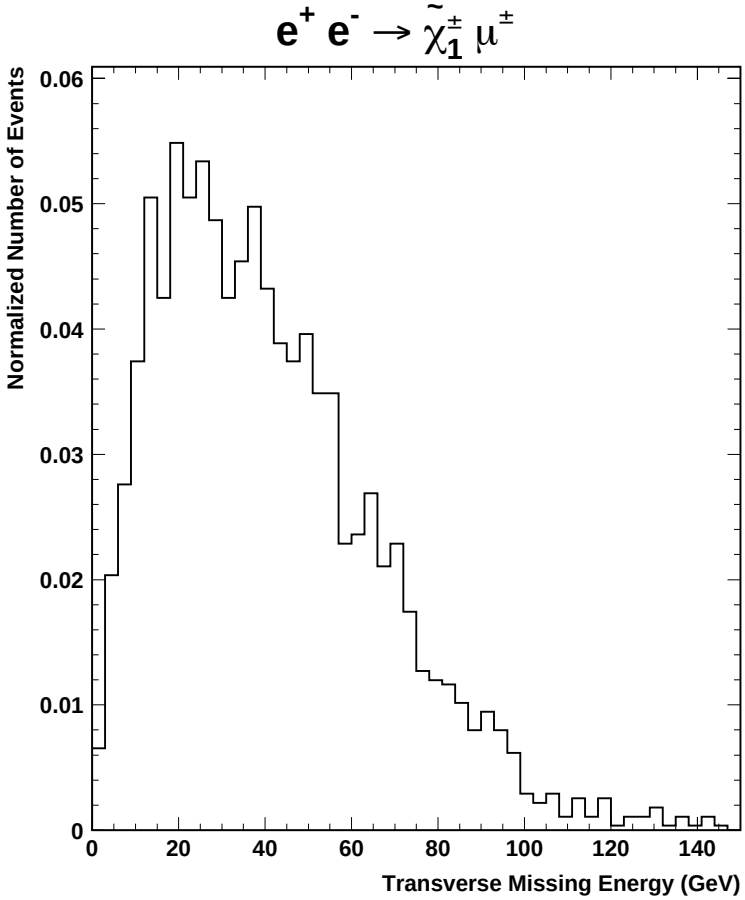

Figure 2: *Distribution of the transverse missing energy (in GeV) in the $4l+\not{E}$ events generated by the single $\tilde{\chi}_1^{\pm}$ production at a center of mass energy of $500GeV$ and for the point A of the SUSY parameter space with $m_{\tilde{\nu}} = 240GeV$. The number of events has been normalized to unity.*

$$e^+e^- \to \tilde{\chi}_i^0 + \tilde{\chi}_j^0 \to \tilde{\chi}_1^0\nu_p\bar{\nu}_p + \tilde{\chi}_1^0\nu_{p'}\bar{\nu}_{p'}, \tag{7}$$

where $i, j = 2, 3, 4$ and $p, p' = 1, 2, 3$. Besides, the pair productions of neutralinos followed by their $\not{R}_p$ decays through λ_{121}:

$$e^+e^- \to \tilde{\chi}_i^0 + \tilde{\chi}_1^0 \to l\bar{l}\nu + \tilde{\chi}_1^0, \tag{8}$$

$$e^+e^- \to \tilde{\chi}_i^0 + \tilde{\chi}_j^0 \to l\bar{l}\nu + \tilde{\chi}_1^0\nu_p\bar{\nu}_p, \tag{9}$$

$$e^+e^- \to \tilde{\chi}_i^0 + \tilde{\chi}_j^0 \to l\bar{l}\nu + l\bar{l}\nu, \tag{10}$$

where $i, j = 2, 3, 4$, are also a source of background.

Secondly, the $4l + \not{E}$ signature can arise in the sneutrino pair production through the reactions,

$$e^+e^- \to \tilde{\nu}_p + \tilde{\nu}_p^* \to \tilde{\chi}_i^0\nu_p + \tilde{\chi}_j^0\bar{\nu}_p, \tag{11}$$

where $i, j = 1, ..., 4$, if the produced neutralinos decay as above, namely either as $\tilde{\chi}_i^0 \to \tilde{\chi}_1^0\nu_p\bar{\nu}_p$ (if $i \neq 1$) or as $\tilde{\chi}_i^0 \to l\bar{l}\nu$.

The neutralinos and sneutrinos pair productions also lead to the $4l + \not{E}$ final state via more complex cascade decays such as $\tilde{\chi}_i^0 \to \tilde{\chi}_j^0 \nu_p \bar{\nu}_p \to \tilde{\chi}_1^0 \nu_{p'} \bar{\nu}_{p'} \nu_p \bar{\nu}_p$ $(i, j = 2, 3, 4$ and $i > j)$ or $\tilde{\nu} \to l^{\mp} \tilde{\chi}_1^{\pm} \to l^{\mp} e^{\pm} \nu_e \nu_\mu$ where the chargino decays through the λ_{121} coupling.

At the high energies available at linear colliders [45, 46], the rates of the neutralinos and sneutrinos pair productions (see Section 5.2.2) are typically quite larger than the cross sections of the Standard Model background reactions (see Section 4.2). We however note that in the regions of large $\tilde{\chi}_i^0$ and $\tilde{\nu}_p$ masses with respect to the center of mass energy $\sqrt{s}$, the $\tilde{\chi}_i^0 \tilde{\chi}_j^0$ and $\tilde{\nu}_p \tilde{\nu}_p^*$ productions cross sections, respectively, are suppressed by the phase space factor. In the kinematic domain $2m_{\tilde{\chi}_i^0}, 2m_{\tilde{\nu}_p} > \sqrt{s} > m_{\tilde{\chi}_1^{\pm}} > m_{\tilde{\chi}_1^0}$ $(i = 1, ..., 4$ and $p = 1, 2, 3)$, all the neutralinos and sneutrinos pair productions are even kinematically closed while the single chargino production remains possible. In such a situation, the only background to the $4l + \not{E}$ final state would be the Standard Model background so that the sensitivity on the λ_{121} coupling would be greatly improved. Nevertheless, the kinematic domain described above is restrictive and not particularly motivated. As a conclusion, except in some particular kinematic domains, the main background to the $4l + \not{E}$ final state is supersymmetric.
In Section 5, we will focus on the largest allowed SUSY background. Indeed, the various considered domains of the SUSY parameter space will be chosen such that the $\tilde{\chi}_1^0$ mass is around the value $m_{\tilde{\chi}_1^0} \approx 100 GeV$ which is close to the experimental limit $m_{\tilde{\chi}_1^0} > 52 GeV$ (for $\tan\beta = 20$ and any λ_{ijk} coupling) [24] in order to maximize the phase space factors of the $\tilde{\chi}_i^0 \tilde{\chi}_j^0$ productions and the decays $\tilde{\nu}_p \to \tilde{\chi}_i^0 \nu_p$.

The SUSY background could be suppressed by the cut on the lepton momentum mentioned in Section 3. The selection of initial leptons of same helicities would also reduce the SUSY background. Indeed, the neutralino (sneutrino) pair production occurs through the exchange of either a Z-boson in the s channel or a charged slepton (chargino) in the t channel, and the helicities of the initial electron and positron are opposite in all those channels. The t channels of the SUSY background processes allow however same helicity leptons in the initial state but this contribution entails the higgsino component of the relevant gaugino and is thus suppressed by powers of $m_l/(m_W \cos\beta)$.

5 Analysis

In this part, we determine the sensitivity on the λ_{121} coupling constant expected from the study of the single chargino production $e^+e^- \to \tilde{\chi}_1^{\pm} \mu^{\mp}$ based on the analysis of the $4l + \not{E}$ final state at linear colliders, assuming a center of mass energy of $\sqrt{s} = 500 GeV$ and a luminosity of $\mathcal{L} = 500 fb^{-1}$. For this purpose, we study the SUSY background and show how it can be reduced with respect to the signal. At the end of this part, we also discuss the determination of the $\tilde{\chi}_1^{\pm}$, $\tilde{\chi}_2^{\pm}$ and $\tilde{\nu}$ masses, the single chargino production at different center of mass energies and via other $\not{R}_p$ couplings, the $3l + 2j + \not{E}$ final state and the single neutralino production.

We have simulated the signal and the supersymmetric background with the new version of the SUSYGEN event generator [47] including the beam polarization effects.

5.1 Polarization

The signal-to-noise ratio could be enhanced by making use of the capability of the linear colliders to polarize the inital beams.

First, as we have seen in Section 4.3 the SUSY background would be reduced if initial leptons of similar helicities were selected. Hence, we consider in this study the selection of the $e_L^- e_L^+$ initial state, namely Left-handed initial electron and positron. In order to illustrate the effect of this polarization on the SUSY background, let us consider for example the $\tilde{\chi}_1^0 \tilde{\chi}_2^0$ production. At the point A of the SUSY parameter space, the unpolarized cross section is $\sigma(e^+e^- \to \tilde{\chi}_1^0 \tilde{\chi}_2^0) = 153.99 fb$ for a center of mass energy of $\sqrt{s} = 500 GeV$. Selecting now the $e_L^- e_L^+$ initial beams and assuming a value of 85% (60%) for the electron (positron) polarization, the production rate becomes $\sigma_{polar}(e^+e^- \to \tilde{\chi}_1^0 \tilde{\chi}_2^0) = 82.56 fb$.

Secondly, the selection of same helicities initial leptons would increase the signal rate as mentioned in Section 3. We discuss here the effect of the considered $e_L^- e_L^+$ beam polarization on the signal rate. As explained in Section 3, the single chargino production occurs through the process $e_L^- e_L^+ \to \tilde{\chi}_1^- \mu^+$ (see Fig.1) or through its charge conjugated process $e_R^- e_R^+ \to \tilde{\chi}_1^+ \mu^-$. These charge conjugated processes have the same cross section: $\sigma(e_L^- e_L^+ \to \tilde{\chi}_1^- \mu^+) = \sigma(e_R^- e_R^+ \to \tilde{\chi}_1^+ \mu^-)$. The whole cross section is thus $\sigma = [\sigma(e_L^- e_L^+ \to \tilde{\chi}_1^- \mu^+) + \sigma(e_R^- e_R^+ \to \tilde{\chi}_1^+ \mu^-)]/4 = \sigma(e_L^- e_L^+ \to \tilde{\chi}_1^- \mu^+)/2$. The chosen beam polarization

favoring Left-handed initial leptons, only the process $e^-_L e^+_L \to \tilde{\chi}^-_1 \mu^+$ would be selected if the polarization were total. The polarized cross section would then be $\sigma^{total}_{polar} = \sigma(e^-_L e^+_L \to \tilde{\chi}^-_1 \mu^+) = 2\ \sigma$. Hence, the signal would be increased by a factor of 2 with respect to the whole cross section. In fact, due to the limited expected efficiency of the beam polarization, the chargino production can also receive a small contribution from the process $e^-_R e^+_R \to \tilde{\chi}^+_1 \mu^-$. The polarized cross section is thus replaced by $\sigma_{polar} = \sigma_{polar}(\tilde{\chi}^-_1 \mu^+) + \sigma_{polar}(\tilde{\chi}^+_1 \mu^-)$ where $\sigma_{polar}(\tilde{\chi}^-_1 \mu^+) = P(e^-_L)P(e^+_L)\sigma(e^-_L e^+_L \to \tilde{\chi}^-_1 \mu^+)$ and $\sigma_{polar}(\tilde{\chi}^+_1 \mu^-) = P(e^-_R)P(e^+_R)\sigma(e^-_R e^+_R \to \tilde{\chi}^+_1 \mu^-)$, $P(e^+_L)$ being for example the probability to have a Left-handed initial positron. Assuming a polarization efficiency of 85% (60%) for the electron (positron) and selecting Left-handed initial leptons, the probabilities are $P(e^-_L) = (1 + 0.85)/2 = 0.925$, $P(e^+_L) = (1 + 0.60)/2 = 0.8$, $P(e^-_R) = (1 - 0.85)/2 = 0.075$ and $P(e^+_R) = (1 - 0.60)/2 = 0.2$. Hence, the polarized cross section reads as $\sigma_{polar} = [P(e^-_L)P(e^+_L) + P(e^-_R)P(e^+_R)]\sigma(e^-_L e^+_L \to \tilde{\chi}^-_1 \mu^+) = 0.755\ \sigma(e^-_L e^+_L \to \tilde{\chi}^-_1 \mu^+) = 1.51\ \sigma$. The signal rate is thus enhanced by a factor of 1.51 with respect to the whole cross section if the $e^-_L e^+_L$ beam polarization is applied.

5.2 Cross sections and branching ratios

5.2.1 Signal

The single $\tilde{\chi}^\pm_1$ chargino production has a cross section typically of order $10fb$ at $\sqrt{s} = 500GeV$ for $\lambda_{121} = 0.05$ [44]. The single $\tilde{\chi}^\pm_1$ production rate is reduced in the higgsino dominated region $|\mu| \ll M_1, M_2$ where the $\tilde{\chi}^\pm_1$ is dominated by its higgsino component, compared to the wino dominated domain $|\mu| \gg M_1, M_2$ in which the $\tilde{\chi}^\pm_1$ is mainly composed by the charged higgsino [44]. Besides, the single $\tilde{\chi}^\pm_1$ production cross section depends weakly on the sign of the μ parameter at large values of $\tan\beta$. However, as $\tan\beta$ decreases the rate increases (decreases) for $sign(\mu) > 0$ (< 0). This evolution of the rate with the $\tan\beta$ and $sign(\mu)$ parameters is explained by the evolution of the $\tilde{\chi}^\pm_1$ mass in the SUSY parameter space [44]. Finally, when the sneutrino mass approaches the resonance ($m_{\tilde{\nu}} = \sqrt{s}$) by lower values, the single $\tilde{\chi}^\pm_1$ production cross section is considerably increased due to the ISR effect [43]. For instance, at the point A of the SUSY parameter space, the rate is equal to $\sigma(e^+e^- \to \tilde{\chi}^\pm_1 \mu^\mp) = 353.90fb$ for a center of mass energy of $\sqrt{s} = 500GeV$ and a sneutrino mass of $m_{\tilde{\nu}} = 240GeV$. At the resonance, the single chargino production rate reaches high values. For example at $m_{\tilde{\nu}} = \sqrt{s} = 500GeV$, the cross section is $\sigma(e^+e^- \to \tilde{\chi}^\pm_1 \mu^\mp) = 30.236pb$ for the same MSSM point A.

Since we consider the $4l + \not{E}$ final state and the chargino width is neglected, the single chargino production rate must be multiplied by the branching ratio of the leptonic chargino decay $B(\tilde{\chi}^\pm_1 \to \tilde{\chi}^0_1 l_p \nu_p)$ ($p = 1, 2, 3$). The leptonic decay of the chargino is typically of order 30% for $m_{\tilde{\nu}}, m_{\tilde{l}^\pm}, m_{\tilde{q}} > m_{\tilde{\chi}^\pm_1}$. This leptonic decay is suppressed compared to the hadronic decay $\tilde{\chi}^\pm_1 \to \tilde{\chi}^0_1 d_p u_{p'}$ ($p = 1, 2, 3; p' = 1, 2$) because of the color factor. Indeed for $m_{\tilde{\nu}}, m_{\tilde{l}^\pm}, m_{\tilde{q}} > m_{\tilde{\chi}^\pm_1}$ the hadronic decay is typically $B(\tilde{\chi}^\pm_1 \to \tilde{\chi}^0_1 d_p u_{p'}) \approx 70\%$ ($p = 1, 2, 3; p' = 1, 2$). In the case where $m_{\tilde{q}} > m_{\tilde{\chi}^\pm_1} > m_{\tilde{\nu}}, m_{\tilde{l}^\pm}$, the decay $\tilde{\chi}^\pm_1 \to \tilde{\chi}^0_1 l_p \nu_p$ occurs through the two-body decays $\tilde{\chi}^\pm_1 \to \tilde{\nu} l^\pm$ and $\tilde{\chi}^\pm_1 \to \tilde{l}^\pm \nu$ and is thus the dominant channel. In such a scenario, the branching ratio of the $4l + \not{E}$ final state for the single $\tilde{\chi}^\pm_1$ production is close to 100%. In contrast, for $m_{\tilde{\nu}}, m_{\tilde{l}^\pm} > m_{\tilde{\chi}^\pm_1} > m_{\tilde{q}}$, the decay $\tilde{\chi}^\pm_1 \to \tilde{\chi}^0_1 d_p u_{p'}$ dominates, as it occurs through the two-body decay $\tilde{\chi}^\pm_1 \to \tilde{q} q'$, and the signal is negligible. The $\not{R}_p$ decays of the chargino via λ_{121}, $\tilde{\chi}^\pm_1 \to e^\pm \mu^\pm e^\mp$, $e^\pm \nu_e \nu_\mu$, have generally negligible branching fractions due to the small values of the $\not{R}_p$ coupling constants. Nevertheless, in the case of nearly degenerate $\tilde{\chi}^\pm_1$ and $\tilde{\chi}^0_1$ masses, those $\not{R}_p$ decays can become dominant spoiling then the $4l + \not{E}$ signature.

5.2.2 SUSY background

In this part, we discuss the variations and the order of magnitude of the cross sections and branching ratios on which the whole SUSY background depends.

• **Neutralino pair production** The neutralinos pair productions represent a SUSY background for the present study of the R-parity violation. A detailed description of the neutralinos pair productions cross sections at linear colliders for an energy of $\sqrt{s} = 500GeV$ has recently been performed in [2]. In order to consider in our analysis the main variations of the neutralinos pair productions rates, we have generated all the $\tilde{\chi}^0_i \tilde{\chi}^0_j$ productions (i and j both varying between 1 and 4) at some points belonging to characteristic regions of the MSSM parameter space. The points chosen for the analysis respect the experimental limits derived from the LEP data on the lightest chargino and neutralino masses, $m_{\tilde{\chi}^0_1} > 52GeV$ ($\tan\beta = 20$)

and $m_{\tilde{\chi}_1^\pm} > 94GeV$ [24], as well as the excluded regions in the $\mu - M_2$ plane [24]. Besides, since the neutralinos pair productions rates depend weakly on $\tan\beta$ and $sign(\mu)$ [2], we have fixed those SUSY parameters at $\tan\beta = 3$ and $sign(\mu) > 0$.

We present now the characteristic domains of the MSSM parameter space considered in our analysis. For each of those domains, we will describe the behaviour of all the $\tilde{\chi}_i^0\tilde{\chi}_j^0$ productions cross sections except the $\tilde{\chi}_i^0\tilde{\chi}_4^0$ productions ($i = 1, ..., 4$). This is justified by the fact that at a center of mass energy of $500GeV$, the dominant neutralinos productions are the $\tilde{\chi}_1^0\tilde{\chi}_1^0$, $\tilde{\chi}_1^0\tilde{\chi}_2^0$ and $\tilde{\chi}_2^0\tilde{\chi}_2^0$ productions in most parts of the SUSY parameter space. We will also discuss in each of the considered regions the values of the branching ratios $B(\tilde{\chi}_2^0 \to \tilde{\chi}_1^0\nu_p\bar{\nu}_p)$ and $B(\tilde{\chi}_2^0 \to l\bar{l}\nu)$ (for $\lambda_{121} = 0.05$) which determine the contribution of the $\tilde{\chi}_1^0\tilde{\chi}_2^0$ and $\tilde{\chi}_2^0\tilde{\chi}_2^0$ productions to the $4l + \not{E}$ signature. The restriction of the discussion to the $\tilde{\chi}_2^0$ decays is justified by the hierarchy mentioned above between the $\tilde{\chi}_i^0\tilde{\chi}_j^0$ productions rates, and by the fact that the $\tilde{\chi}_3^0$ and $\tilde{\chi}_4^0$ cascade decays have many possible combinations, due to the large $\tilde{\chi}_3^0$ and $\tilde{\chi}_4^0$ masses with respect to the $\tilde{\chi}_1^0$ and $\tilde{\chi}_2^0$ masses, so that the contributions of the $\tilde{\chi}_i^0\tilde{\chi}_j^0$ productions (with i or j equal to 3 or 4) to the $4l + \not{E}$ signature are suppressed by small branching ratio factors. We will also not discuss the complex cascade decays mentioned in Section 4.3 since the associated branching ratios are typically small. However, all the $\tilde{\chi}_i^0\tilde{\chi}_j^0$ productions as well as all the cascade decays of the four neutralinos are taken into account in the analysis.

First, we consider the higgsino dominated region characterised by $|\mu| \ll M_1, M_2$ where the $\tilde{\chi}_1^0$ and $\tilde{\chi}_2^0$ neutralinos are predominantly composed by the higgsinos. In this higgsino region, due to the weak couplings of the higgsinos to charged leptons, the $\tilde{\chi}_1^0\tilde{\chi}_i^0$ and $\tilde{\chi}_2^0\tilde{\chi}_i^0$ productions ($i = 1, 2, 3$) are reduced. However, the $\tilde{\chi}_1^0\tilde{\chi}_2^0$ production rate reaches its larger values in this domain because of the $Z\tilde{\chi}_i^0\tilde{\chi}_j^0$ coupling. At $\sqrt{s} = 500GeV$, the $\tilde{\chi}_3^0\tilde{\chi}_3^0$ production is suppressed by a small phase space factor (when kinematically allowed). For the MSSM point A which belongs to this higgsino region, the cross sections including the beam polarization described in Section 5.1 are $\sigma(\tilde{\chi}_1^0\tilde{\chi}_1^0) = 0.29fb$, $\sigma(\tilde{\chi}_1^0\tilde{\chi}_2^0) = 82.56fb$, $\sigma(\tilde{\chi}_2^0\tilde{\chi}_2^0) = 0.11fb$, $\sigma(\tilde{\chi}_1^0\tilde{\chi}_3^0) = 6.62fb$, $\sigma(\tilde{\chi}_2^0\tilde{\chi}_3^0) = 6.31fb$, $\sigma(\tilde{\chi}_3^0\tilde{\chi}_3^0) = 13.57fb$, $\sigma(\tilde{\chi}_1^0\tilde{\chi}_4^0) = 1.11fb$ and $\sigma(\tilde{\chi}_2^0\tilde{\chi}_4^0) = 9.59fb$ for the kinematically open neutralinos productions at $\sqrt{s} = 500GeV$.
The $\tilde{\chi}_1^0\tilde{\chi}_2^0$ production gives rise to the $4l + \not{E}$ final state if the second lightest neutralino decays as $\tilde{\chi}_2^0 \to \tilde{\chi}_1^0\bar{\nu}_p\nu_p$. In the higgsino region, due to the various decay channels of the $\tilde{\chi}_2^0$, the branching ratio $B(\tilde{\chi}_2^0 \to \tilde{\chi}_1^0\bar{\nu}_p\nu_p)$ reaches values only about 15%. At the point A of the MSSM parameter space, this branching is $B(\tilde{\chi}_2^0 \to \tilde{\chi}_1^0\bar{\nu}_p\nu_p) = 15.8\%$ for $m_{\tilde{\nu}} = 450GeV$. For a $\tilde{\nu}$ lighter than the $\tilde{\chi}_2^0$, the branching $B(\tilde{\chi}_2^0 \to \tilde{\chi}_1^0\bar{\nu}_p\nu_p)$ is enhanced as this decay occurs via the two-body decay $\tilde{\chi}_2^0 \to \tilde{\nu}\nu$. At the point A with $m_{\tilde{\nu}} = 125GeV$, $B(\tilde{\chi}_2^0 \to \tilde{\chi}_1^0\bar{\nu}_p\nu_p) = 62.3\%$.

Secondly, we consider the wino dominated region $|\mu| \gg M_1, M_2$ where $\tilde{\chi}_1^0$ and $\tilde{\chi}_2^0$ are primarily bino and wino, respectively. In this wino region, the $\tilde{\chi}_3^0\tilde{\chi}_i^0$ productions are reduced since the $\tilde{\chi}_3^0$ mass strongly increases with the absolute value of the parameter $|\mu|$. Therefore in the wino region, the main neutralinos productions are the $\tilde{\chi}_1^0\tilde{\chi}_1^0$, $\tilde{\chi}_1^0\tilde{\chi}_2^0$ and $\tilde{\chi}_2^0\tilde{\chi}_2^0$ productions. In this part of the MSSM parameter space and for $m_{\tilde{l}^\pm} = 300GeV$, the $\tilde{\chi}_1^0\tilde{\chi}_1^0$ production can reach $\sim 30fb$, after the beam polarization described in Section 5.1 has been applied. Moreover in this region, while the $\tilde{\chi}_1^0\tilde{\chi}_2^0$ production cross section is typically smaller than the $\tilde{\chi}_1^0\tilde{\chi}_1^0$ production rate, the $\tilde{\chi}_2^0\tilde{\chi}_2^0$ production cross section can reach higher values. At the point B belonging to this wino region and defined as $M_1 = 100GeV$, $M_2 = 200GeV$, $\mu = 600GeV$, $\tan\beta = 3$, $m_{\tilde{l}^\pm} = 300GeV$ and $m_{\tilde{q}} = 600GeV$ ($m_{\tilde{\chi}_1^\pm} = 189.1GeV$, $m_{\tilde{\chi}_1^0} = 97.3GeV$, $m_{\tilde{\chi}_2^0} = 189.5GeV$), the cross sections (including the beam polarization described in Section 5.1) for the allowed neutralinos productions at $\sqrt{s} = 500GeV$ are $\sigma(\tilde{\chi}_1^0\tilde{\chi}_1^0) = 32.21fb$, $\sigma(\tilde{\chi}_1^0\tilde{\chi}_2^0) = 25.60fb$ and $\sigma(\tilde{\chi}_2^0\tilde{\chi}_2^0) = 26.40fb$.
In the wino region and for $M_1 < M_2$, the difference between the $\tilde{\chi}_2^0$ and the $\tilde{\chi}_1^0$ masses increases with $|\mu|$ [44] and can reach high values. Thus, the decay $\tilde{\chi}_2^0 \to \tilde{\chi}_1^0 + Z^0$ is often dominant. At the point B and with $m_{\tilde{\nu}} = 450GeV$, this channel has a branching fraction of $B(\tilde{\chi}_2^0 \to \tilde{\chi}_1^0 Z^0) = 79.9\%$. The decay of the Z-boson into neutrinos has a branching fraction of $B(Z^0 \to \nu_p\bar{\nu}_p) = 20.0\%$. In the wino region and for $M_1 > M_2$, the mass difference $m_{\tilde{\chi}_2^0} - m_{\tilde{\chi}_1^\pm}$ is larger than the $W^\pm$ mass as long as $M_1 - M_2$ is larger than $\sim 75GeV$. In this case, the dominant channel is $\tilde{\chi}_2^0 \to \tilde{\chi}_1^\pm W^\mp$. For $M_1 - M_2$ smaller than $\sim 75GeV$, $m_{\tilde{\chi}_2^0} - m_{\tilde{\chi}_1^\pm}$ remains large enough to allow a dominant decay of type $\tilde{\chi}_2^0 \to \tilde{\chi}_1^\pm f\bar{f}$, f being a fermion. As a conclusion, in the wino region the decay $\tilde{\chi}_2^0 \to \tilde{\chi}_1^0\bar{\nu}_p\nu_p$ can have a significant branching ratio for $M_1 < M_2$.

We also consider some intermediate domains. At the point C defined as $M_1 = 100GeV$, $M_2 = 400GeV$, $\mu = 400GeV$, $\tan\beta = 3$, $m_{\tilde{l}^\pm} = 300GeV$ and $m_{\tilde{q}} = 600GeV$ ($m_{\tilde{\chi}_1^\pm} = 329.9GeV$, $m_{\tilde{\chi}_1^0} = 95.5GeV$, $m_{\tilde{\chi}_2^0} = 332.3GeV$) with $m_{\tilde{\nu}} = 450GeV$, the cross sections (including beam polarization) for the allowed

neutralinos productions at $\sqrt{s} = 500GeV$ are $\sigma(\tilde{\chi}_1^0\tilde{\chi}_1^0) = 32.18fb$, $\sigma(\tilde{\chi}_1^0\tilde{\chi}_2^0) = 6.64fb$ and $\sigma(\tilde{\chi}_1^0\tilde{\chi}_3^0) = 0.17fb$, and the branching ratio of the $\tilde{\chi}_2^0$ decay into neutrinos is $B(\tilde{\chi}_2^0 \to \tilde{\chi}_1^0\bar{\nu}_p\nu_p) = 0.9\%$. The branching ratio of the decay $\tilde{\chi}_2^0 \to \tilde{\chi}_1^0\bar{\nu}_p\nu_p$ is small for this point C since the $\tilde{\chi}_2^0$ mass is large which favors other $\tilde{\chi}_2^0$ decays.

At the point D given by $M_1 = 150GeV$, $M_2 = 300GeV$, $\mu = 200GeV$, $\tan\beta = 3$, $m_{\tilde{l}^\pm} = 300GeV$ and $m_{\tilde{q}} = 600GeV$ ($m_{\tilde{\chi}_1^\pm} = 165.1GeV$, $m_{\tilde{\chi}_1^0} = 121.6GeV$, $m_{\tilde{\chi}_2^0} = 190.8GeV$), the cross sections (including beam polarization) for the allowed neutralinos productions at $\sqrt{s} = 500GeV$ are $\sigma(\tilde{\chi}_1^0\tilde{\chi}_1^0) = 7.80fb$, $\sigma(\tilde{\chi}_1^0\tilde{\chi}_2^0) = 13.09fb$, $\sigma(\tilde{\chi}_2^0\tilde{\chi}_2^0) = 10.08fb$, $\sigma(\tilde{\chi}_1^0\tilde{\chi}_3^0) = 35.69fb$, $\sigma(\tilde{\chi}_2^0\tilde{\chi}_3^0) = 41.98fb$, $\sigma(\tilde{\chi}_3^0\tilde{\chi}_3^0) = 0.02fb$ and $\sigma(\tilde{\chi}_1^0\tilde{\chi}_4^0) = 0.42fb$. Since this point D lies in a particular region between the higgsino region and the domain of large $|\mu|$ (or equivalently large $m_{\tilde{\chi}_3^0}$), the $\tilde{\chi}_1^0\tilde{\chi}_3^0$ and $\tilde{\chi}_2^0\tilde{\chi}_3^0$ productions become relatively important. At the MSSM point D and for $m_{\tilde{\nu}} = 450GeV$, the branching ratio of the $\tilde{\chi}_2^0$ decay into neutrinos is $B(\tilde{\chi}_2^0 \to \tilde{\chi}_1^0\bar{\nu}_p\nu_p) = 10.6\%$.

Finally, in the domain of low charged slepton masses the $\tilde{\chi}_i^0\tilde{\chi}_j^0$ productions are increased due to the t channel $\tilde{l}^\pm$ exchange contribution. At the point E, defined as the point B with a lower $\tilde{l}^\pm$ mass, namely $M_1 = 100GeV$, $M_2 = 200GeV$, $\mu = 600GeV$, $\tan\beta = 3$, $m_{\tilde{l}^\pm} = 150GeV$ and $m_{\tilde{q}} = 600GeV$, the polarized neutralinos pair productions rates which read as $\sigma(\tilde{\chi}_1^0\tilde{\chi}_1^0) = 67.06fb$, $\sigma(\tilde{\chi}_1^0\tilde{\chi}_2^0) = 57.15fb$ and $\sigma(\tilde{\chi}_2^0\tilde{\chi}_2^0) = 69.56fb$ are increased compared to the point B.
For $m_{\tilde{\chi}_2^0} > m_{\tilde{l}^\pm}$ or $m_{\tilde{\chi}_2^0} > m_{\tilde{q}}$, the dominant $\tilde{\chi}_2^0$ decays are $\tilde{\chi}_2^0 \to \tilde{\chi}_1^0\bar{l}_p l_p$ or $\tilde{\chi}_2^0 \to \tilde{\chi}_1^0\bar{q}_p q_p$, respectively, and the decay $\tilde{\chi}_2^0 \to \tilde{\chi}_1^0\bar{\nu}_p\nu_p$ is typically negligible except for $m_{\tilde{\chi}_2^0} > m_{\tilde{\nu}}$. At the point E for $m_{\tilde{\nu}} > m_{\tilde{\chi}_2^0}$, the $\tilde{\chi}_2^0$ mainly decays into $\tilde{\chi}_1^0\bar{l}_p l_p$ via an on shell $\tilde{l}_p^\pm$ and the decay into neutrinos has a branching ratio of $B(\tilde{\chi}_2^0 \to \tilde{\chi}_1^0\bar{\nu}_p\nu_p) \sim 0\%$. In contrast, at the point E with $m_{\tilde{\nu}} = 160GeV$, $B(\tilde{\chi}_2^0 \to \tilde{\chi}_1^0\bar{\nu}_p\nu_p) = 32.0\%$. Of course for $m_{\tilde{l}^\pm}, m_{\tilde{q}} > m_{\tilde{\chi}_2^0} > m_{\tilde{\nu}}$, the decay $\tilde{\chi}_2^0 \to \tilde{\chi}_1^0\bar{\nu}_p\nu_p$ is dominant.

• **Sneutrino pair production** The other source of SUSY background is the sneutrino pair production. We discuss here the main variations of this background in the SUSY parameter space. First, we note that the $\tilde{\nu}_1$ pair production has the highest cross section among the $\tilde{\nu}_p\tilde{\nu}_p^*$ ($p = 1, 2, 3$ being the family index) productions since it receives a contribution from the t channel exchange of charginos. Besides, the main contribution to the $4l + \not{E}$ signature from the sneutrino pair production is the reaction $e^+e^- \to \tilde{\nu}_p + \tilde{\nu}_p^* \to \tilde{\chi}_1^0\nu_p + \tilde{\chi}_1^0\bar{\nu}_p$. Indeed, this contribution has the simplest cascade decays and furthermore the decay $\tilde{\nu}_p \to \tilde{\chi}_1^0\nu_p$ is favored by the phase space factor. Hence, we restrict the discussion of the $\tilde{\nu}_p\tilde{\nu}_p^*$ background to this reaction, although all contributions from the sneutrino pair productions to the $4l + \not{E}$ signature are included in our analysis.

The $\tilde{\nu}_p$ pair production rate is reduced in the higgsino region like the $\tilde{\chi}_1^0\tilde{\chi}_1^0$ production. For instance, at the point A with $m_{\tilde{\nu}} = 175GeV$ the sneutrino pair production cross section including the beam polarization effect described in Section 5.1 is $\sigma(e^+e^- \to \tilde{\chi}_1^0\nu_p\tilde{\chi}_1^0\bar{\nu}_p) = 75.26fb$ ($1.96fb$) for $p = 1$ ($2, 3$), while it is $\sigma(e^+e^- \to \tilde{\chi}_1^0\nu_p\tilde{\chi}_1^0\bar{\nu}_p) = 501.55fb$ ($10.29fb$) for $p = 1$ ($2, 3$) at the point B with the same sneutrino mass. These values of the cross sections are obtained with SUSYGEN [47] and include the spin correlations effect. Besides, the $\tilde{\nu}_p$ pair production rates strongly decrease as the sneutrino mass increases. Considering once more the point B, we find that the rate is reduced to $\sigma(e^+e^- \to \tilde{\chi}_1^0\nu_p\tilde{\chi}_1^0\bar{\nu}_p) = 232.92fb$ ($4.59fb$) for $p = 1$ ($2, 3$) if we take now $m_{\tilde{\nu}} = 200GeV$.
The branching ratio $B(\tilde{\nu} \to \tilde{\chi}_1^0\nu)$ decreases as the sneutrino mass increases, since the phase space factors associated to the decays of the sneutrino into other SUSY particles than the $\tilde{\chi}_1^0$, like $\tilde{\nu} \to \tilde{\chi}_1^\pm l^\mp$, increase with $m_{\tilde{\nu}}$. For example, at the point B the branching ratio $B(\tilde{\nu}_e \to \tilde{\chi}_1^0\nu_e)$ is equal to 93.4% for $m_{\tilde{\nu}} = 175GeV$ and to 82.6% for $m_{\tilde{\nu}} = 200GeV$.

5.3 Cuts

5.3.1 General selection criteria

First, we select the events without jets containing 4 charged leptons and missing energy. In order to take into account the observability of leptons at a $500GeV$ e^+e^- machine, we apply the following cuts on the transverse momentum and rapidity of all the charged leptons: $P_t(l) > 3GeV$ and $|\eta(l)| < 3$. This should simulate the detector acceptance effects in a first approximation. In order to reduce the supersymmetric background, we also demand that the number of muons is at least equal to one. Since we consider the $\tilde{\chi}_1^\pm\mu^\mp$ production, this does not affect the signal.

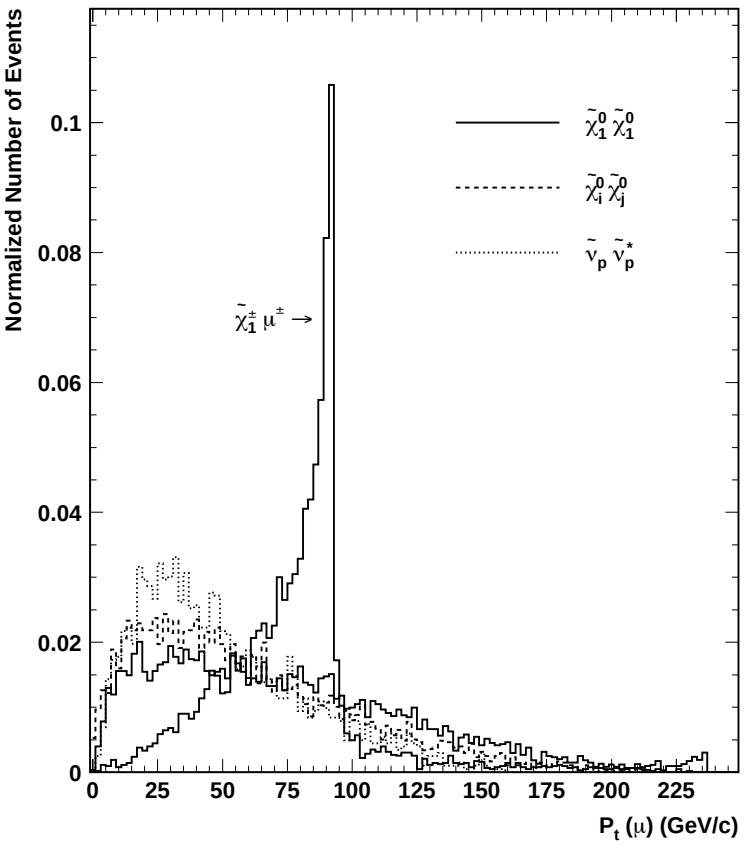

Figure 3: *Distributions of the highest muon transverse momentum $P_t(\mu)$ (in GeV/c) for the $4l + \not{E}$ events generated by the single $\tilde{\chi}_1^{\pm}$ production and the SUSY background which is divided into the $\tilde{\chi}_1^0\tilde{\chi}_1^0$, $\tilde{\chi}_i^0\tilde{\chi}_j^0$ and $\tilde{\nu}_p\tilde{\nu}_p^*$ productions. The number of events for each distribution is normalized to the unity, the center of mass energy is fixed at $500GeV$ and the point A of the SUSY parameter space is considered with $\lambda_{121} = 0.05$ and $m_{\tilde{\nu}} = 240GeV$.*

5.3.2 Kinematics of the muon produced with the chargino

We now discuss in details the most important cut concerning the momentum of the muon which is produced together with the chargino. For a negligible ISR effect, this muon momentum is completely determined by the values of the chargino mass and the center of mass energy through Eq.(4), as explained in Section 3. Hence, some cuts on the muon momentum should be efficient to enhance the signal-to-noise ratio since the muon momentum distribution is perfectly peaked at a given value.
For a significant ISR effect, the energy of the photon generated via the ISR must be taken into account. Hence, the muon energy $E(\mu)$ must be calculated through the three-body kinematics of the reaction $e^+e^- \rightarrow \tilde{\chi}_1^{\pm}\mu^{\mp}\gamma$. Since this kinematics depends on the angle between the muon and the photon, the muon energy $E(\mu)$ is not completely fixed by the SUSY parameters anymore. Therefore, the distribution obtained experimentally of the muon momentum $P(\mu) = (E(\mu)^2 - m_{\mu^{\pm}}^2 c^4)^{1/2}/c$ would appear as a peaked curve instead of a Dirac peak. Although the momentum of the produced muon remains a good selection criteria, we have found that in this case the transverse momentum distribution of the produced muon was more peaked, and thus more appropriate to apply some cuts. We explain the reasons why in details below.
We have thus chosen to apply cuts on the distribution of the muon transverse momentum instead of the whole muon momentum, even if for a negligible ISR effect the transverse momentum distribution is not

peaked as well as the whole momentum distribution. The amplitude of the ISR effect depends on the SUSY mass spectrum as we will discuss below.
The cuts on the muon transverse momentum have been applied on the muon with the highest transverse momentum which can be identified as the muon produced together with the chargino in the case of the signal. Indeed, the muon produced together with the chargino is typically more energetic than the 3 other leptons generated in the chargino cascade decay. We will come back on this point later.

In Fig.3, we show the distribution of the highest muon transverse momentum $P_t(\mu)$ in the $4l + \not{E}$ events generated by the single $\tilde{\chi}_1^{\pm}$ production and the SUSY background at $\sqrt{s} = 500GeV$ for the point A of the SUSY parameter space with $\lambda_{121} = 0.05$ and $m_{\tilde{\nu}} = 240GeV$. For these SUSY parameters, the cross sections, polarized as in Section 5.1, and the branching ratios are $\sigma(\tilde{\chi}_1^{\pm}\mu^{\mp}) = 534.39fb$, $B(\tilde{\chi}_1^{\pm} \rightarrow \tilde{\chi}_1^0 l_p \nu_p) = 34.3\%$, $\sigma(e^+e^- \rightarrow \tilde{\nu}_p + \tilde{\nu}_p^* \rightarrow \tilde{\chi}_1^0\nu_p + \tilde{\chi}_1^0\bar{\nu}_p) = 3.81fb$ and $B(\tilde{\chi}_2^0 \rightarrow \tilde{\chi}_1^0\bar{\nu}_p\nu_p) = 16\%$ (see Section 5.2.2 for the values of $\sigma(\tilde{\chi}_i^0\tilde{\chi}_j^0)$). In Fig.3, the cuts described in Section 5.3.1 have not been applied and in order to perform a separate analysis for each of the main considered backgrounds, the SUSY background has been decomposed into three components: the $\tilde{\chi}_1^0\tilde{\chi}_1^0$, $\tilde{\chi}_i^0\tilde{\chi}_j^0$ ($i, j = 1, ..., 4$ with i and j not equal to 1 simultaneously) and $\tilde{\nu}_p\tilde{\nu}_p^*$ productions. The number of $4l + \not{E}$ events for each of those 3 SUSY backgrounds and the single chargino production has been normalized to the unity. Our motivation for such a normalization is that the relative amplitudes of the 3 SUSY backgrounds and the single chargino production, which depend strongly on the SUSY parameters, were discussed in detail in Sections 5.2.1 and 5.2.2, and in this section we focus on the shapes of the various distributions.
We see in the highest muon transverse momentum distribution of Fig.3 that, as expected, a characteristic peak arises for the single chargino production. Therefore, some cuts on the highest muon transverse momentum $P_t(\mu)$ would greatly increase the signal with respect to the backgrounds. For instance, the selection criteria suggested by the Fig.3 are something like $60GeV \lesssim P_t(\mu) \lesssim 100GeV$. We can also observe in Fig.3 that the distributions of the $\tilde{\chi}_i^0\tilde{\chi}_j^0$ and $\tilde{\nu}_p\tilde{\nu}_p^*$ productions are concentrated at lower transverse momentum values than the $\tilde{\chi}_1^0\tilde{\chi}_1^0$ distribution. This is due to the energy carried away by the neutrinos in the cascade decays of the reactions (6), (7), (9) and (11). The main variation of the highest muon transverse momentum distributions of the SUSY backgrounds with the SUSY parameters is the following: The SUSY backgrounds distributions spread to larger values of the muon transverse momentum as the $\tilde{\chi}_1^0$ mass increases, since then the charged leptons coming from the decay $\tilde{\chi}_1^0 \rightarrow l\bar{l}\nu$ reach higher energies.
Fig.3 shows also clearly that the peak in the transverse momentum distribution of the muon produced with the chargino exhibits an upper limit which we note $P_t^{lim}(\mu)$. This bound $P_t^{lim}(\mu)$ is a kinematic limit and thus its value depends on the SUSY masses. The consequence on our analysis is that the cuts on the muon transverse momentum are modified as the SUSY mass spectrum is changing. Note that the kinematic limit of the whole muon momentum depends also on the SUSY masses, so that our choice of working with the transverse momentum remains judicious. For a better understanding of the analysis and in view of the study on the SUSY mass spectrum of Section 5.5, we now determine the value of the muon transverse momentum kinematic limit $P_t^{lim}(\mu)$ as a function of the SUSY parameters. For this purpose we divide the discussion into 2 scenarios.

First, we consider the situation where $m_{\tilde{\nu}_\mu} > m_{\tilde{\chi}_1^{\pm}} + m_{\mu^{\mp}}$ and $m_{\tilde{\nu}_\mu} < \sqrt{s}$. In this case, the dominant s channel contribution to the three-body reaction $e^+e^- \rightarrow \tilde{\chi}_1^{\pm}\mu^{\mp}\gamma$, where the photon is generated by the ISR, can be decomposed into two levels. First, a sneutrino is produced together with a photon in the two-body reaction $e^+e^- \rightarrow \gamma\tilde{\nu}_\mu$ and then the sneutrino decays as $\tilde{\nu}_\mu \rightarrow \tilde{\chi}_1^{\pm}\mu^{\mp}$. Thus, the muon energy in the center of mass of the sneutrino $E^\star(\mu)$ (throughout this article a $\star$ indicates that the variable is defined in the center of mass of the produced sneutrino) is equal to,

$$E^\star(\mu) = \frac{m_{\tilde{\nu}_\mu}^2 + m_\mu^2 - m_{\tilde{\chi}^{\pm}}^2}{2m_{\tilde{\nu}_\mu}}. \tag{12}$$

The transverse momentum limit of the produced muon in the center of mass of the sneutrino $P_t^{lim\star}(\mu)$ is given by $P_t^{lim\star}(\mu) = (E^\star(\mu)^2 - m_{\mu^{\pm}}^2 c^4)^{1/2}/c$ since $P_t^\star(\mu) \leq P^\star(\mu)$ and $P^\star(\mu) = (E^\star(\mu)^2 - m_{\mu^{\pm}}^2 c^4)^{1/2}/c$. The important point is that the sneutrino rest frame is mainly boosted in the direction of the beam axis. This is due to the fact that the produced photon is mainly radiated at small angles with respect to the initial colliding particles direction (see Fig.4). The consequence is that the transverse momentum of the produced muon is mainly the same in the sneutrino rest frame and in the laboratory frame. In conclusion, the transverse momentum limit of the produced muon in the laboratory frame is given by

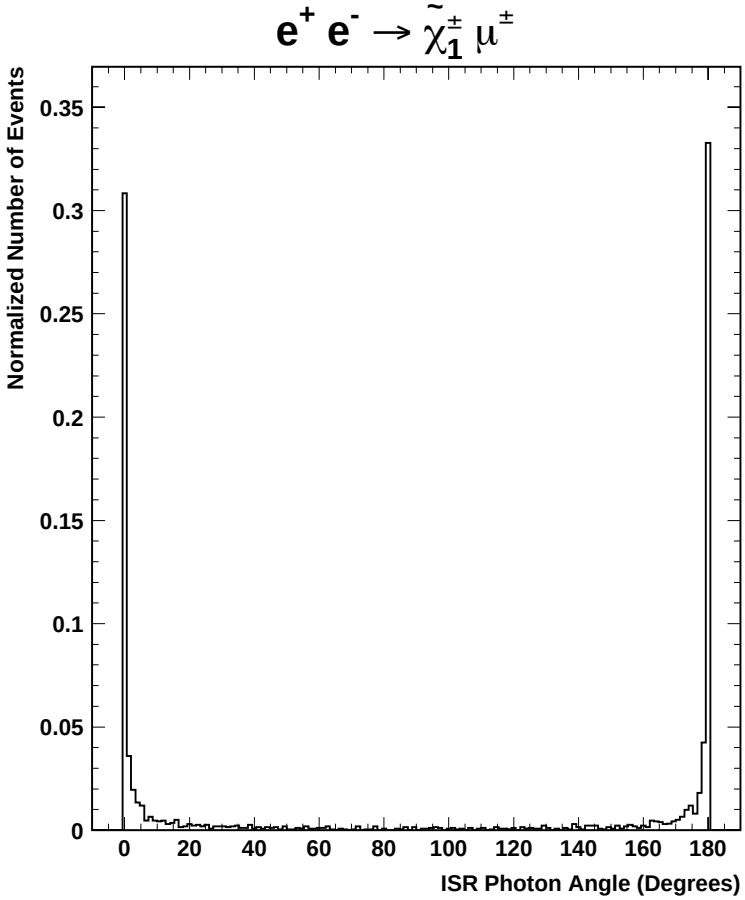

Figure 4: *Distribution of the angle (in Degrees) between the beam axis and the photon radiated from the initial state of the single $\tilde{\chi}_1^{\pm}$ production process at a center of mass energy of $500GeV$ and for the point A of the SUSY parameter space with $m_{\tilde{\nu}} = 240GeV$. The number of events has been normalized to the unity.*

$P_t^{lim}(\mu) \approx P_t^{lim\star}(\mu) = (E^{\star}(\mu)^2 - m_{\mu^{\pm}}^2 c^4)^{1/2}/c$, $E^{\star}(\mu)$ being calculated through Eq.(12). We see explicitly through Eq.(12) that the value of $P_t^{lim}(\mu) \approx (E^{\star}(\mu)^2 - m_{\mu^{\pm}}^2 c^4)^{1/2}/c$ increases with the sneutrino mass. In this first situation, where $m_{\tilde{\nu}_\mu} > m_{\tilde{\chi}_1^{\pm}} + m_{\mu^{\mp}}$ and $m_{\tilde{\nu}_\mu} < \sqrt{s}$, the ISR effect is large so that the single chargino production cross section is enhanced. The distributions of Fig.3 are obtained for the point A (for which $m_{\tilde{\chi}_1^{\pm}} = 115.7GeV$) with $m_{\tilde{\nu}_\mu} = 240GeV$ which corresponds to this situation of large ISR. The distribution of Fig.3 gives a value for the transverse momentum kinematic limit of $P_t^{lim}(\mu) = 92.3GeV/c$ which is well approximately equal to $(E^{\star}(\mu)^2 - m_{\mu^{\pm}}^2 c^4)^{1/2}/c = 92.1GeV/c$ where $E^{\star}(\mu)$ is calculated using Eq.(12).

Based on this explanation, we can now understand why for large ISR the transverse momentum of the produced muon $P_t(\mu)$ is more peaked than its whole momentum $P(\mu)$: As we have discussed above, the muon transverse momentum $P_t(\mu)$ is controlled by the two-body kinematics of the decay $\tilde{\nu}_\mu \to \tilde{\chi}_1^{\pm}\mu^{\mp}$. For a set of SUSY parameters, the muon transverse momentum is thus fixed if only the absolute value of the cosinus of the angle that makes the muon with the initial beam direction in the sneutrino rest frame is given. In contrast, the whole muon momentum $P(\mu)$ is given by the three-body kinematics of the reaction $e^+e^- \to \tilde{\chi}_1^{\pm}\mu^{\mp}\gamma$ and thus depends on the cosinus of the angle between the muon and the photon (recall that the photon is mainly emitted along the beam axis) in the laboratory frame. Therefore, the muon transverse momentum $P_t(\mu)$ is less dependent on the muon angle than the whole muon momentum $P(\mu)$, leading thus to a more peaked distribution.

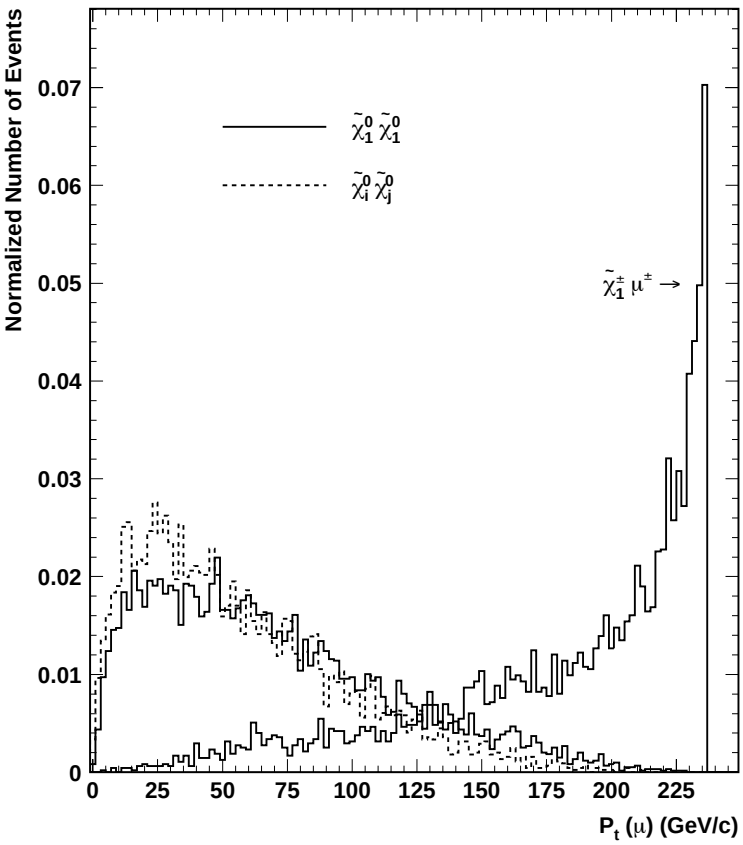

Figure 5: *Distributions of the highest muon transverse momentum $P_t(\mu)$ (in GeV/c) for the $4l + \not{E}$ events generated by the single $\tilde{\chi}_1^\pm$ production and the SUSY background which is divided into the $\tilde{\chi}_1^0\tilde{\chi}_1^0$ and $\tilde{\chi}_i^0\tilde{\chi}_j^0$ productions. The number of events for each distribution is normalized to the unity, the center of mass energy is fixed at $500GeV$ and the point A of the SUSY parameter space is considered with $\lambda_{121} = 0.05$ and $m_{\tilde{\nu}} = 550GeV$.*

We consider now the scenario where $m_{\tilde{\nu}_\mu} < m_{\tilde{\chi}_1^\pm} + m_{\mu^\mp}$ or $m_{\tilde{\nu}_\mu} > \sqrt{s}$. In such a situation, the kinematics is different since the sneutrino cannot be produced on shell. The single chargino production $e^+e^- \rightarrow \tilde{\chi}_1^\pm \mu^\mp \gamma$ can thus not occur through the two-body reaction $e^+e^- \rightarrow \gamma\tilde{\nu}_\mu$. In fact in this situation, the energy of the radiated photon becomes negligible so that the muon energy $E(\mu)$ is given in a good approximation by the two-body kinematics formula of Eq.(4). The kinematic limit of the muon transverse momentum is related to this energy through $P_t^{lim}(\mu) = P(\mu) = (E(\mu)^2 - m_{\mu^\pm}^2 c^4)^{1/2}/c$.
In this second scenario where $m_{\tilde{\nu}_\mu} < m_{\tilde{\chi}_1^\pm} + m_{\mu^\mp}$ or $m_{\tilde{\nu}_\mu} > \sqrt{s}$, the ISR effect is negligible and the single chargino production rate is thus not increased. In Fig.5, we show the transverse momentum distribution (without the cuts of Section 5.3.1) of the produced muon in such a situation, namely at $\sqrt{s} = 500GeV$ for the point A of the SUSY parameter space with $\lambda_{121} = 0.05$ and $m_{\tilde{\nu}_\mu} = 550GeV$. For these SUSY parameters, the cross sections, polarized as in Section 5.1, and the branching ratios are $\sigma(\tilde{\chi}_1^\pm \mu^\mp) = 91.05fb$, $B(\tilde{\chi}_1^\pm \rightarrow \tilde{\chi}_1^0 l_p \nu_p) = 33.9\%$ and $B(\tilde{\chi}_2^0 \rightarrow \tilde{\chi}_1^0 \bar{\nu}_p \nu_p) = 15.7\%$ (see Section 5.2.2 for the values of $\sigma(\tilde{\chi}_i^0\tilde{\chi}_j^0)$. We check that the value of the muon transverse momentum kinematic limit $P_t^{lim}(\mu) = 236.7GeV/c$ obtained from the distribution of Fig.5 is well approximately equal to $(E(\mu)^2 - m_{\mu^\pm}^2 c^4)^{1/2}/c = 236.6GeV/c$ where $E(\mu)$ is obtained from Eq.(4).

At this stage, we can make a comment on the variation of the muon transverse momentum distribution associated to the single $\tilde{\chi}_1^\pm$ production with the value of the transverse momentum limiy $P_t^{lim}(\mu)$. As can

be seen by comparing Fig.3 and Fig.5, this distribution is more peaked for small values of $P_t^{lim}(\mu)$ due to an higher concentration of the distribution at low muon transverse momentum values. This effect is compensated by the fact that at low muon transverse momentum values the SUSY background is larger, as can be seen in Fig.3.

The determination of $P_t^{lim}(\mu)$ performed in this section allows us to verify that the muon produced with the chargino is well often the muon of highest transverse momentum. Indeed, we have checked that in the two situations of large (point A with $m_{\tilde{\nu}_\mu} = 240GeV$) and negligible (point A with $m_{\tilde{\nu}_\mu} = 550GeV$) ISR effect, the calculated values of $P_t^{lim}(\mu)$ for the produced muon were consistent with the values of $P_t^{lim}(\mu)$ obtained with the highest muon transverse momentum distributions (Fig.3 and Fig.5). Therefore, the identification of the produced muon with the muon of highest transverse momentum is correct for the two MSSM points considered above. The well peaked shapes of the highest muon transverse momentum distributions for the point A with $m_{\tilde{\nu}_\mu} = 240GeV$ and $m_{\tilde{\nu}_\mu} = 550GeV$ are another confirmation of the validity of this identification. Nevertheless, one must wonder what is the domain of validity of this identification. In particular, the transverse momentum of the produced muon can be small since $P_t^{lim}(\mu)$ which is determined via Eq.(4) or Eq.(12) can reach low values. As a matter of fact, $P_t^{lim}(\mu)$ can reach small values in the scenario where $m_{\tilde{\nu}_\mu} > m_{\tilde{\chi}_1^\pm} + m_{\mu^\mp}$ and $m_{\tilde{\nu}_\mu} < \sqrt{s}$ for $m_{\tilde{\nu}_\mu}$ close to $m_{\tilde{\chi}_1^\pm}$ (see Eq.(12)), as well as in the scenario where $m_{\tilde{\nu}_\mu} < m_{\tilde{\chi}_1^\pm} + m_{\mu^\mp}$ or $m_{\tilde{\nu}_\mu} > \sqrt{s}$ for $\sqrt{s}$ close to $m_{\tilde{\chi}_1^\pm}$ (see Eq.(4)). Moreover, the leptons generated in the cascade decay initiated by the $\tilde{\chi}_1^\pm$ become more energetic, and can thus have larger transverse momentum, for either larger $\tilde{\chi}_1^0$ masses or higher mass differences between the $\tilde{\chi}_1^\pm$ and $\tilde{\chi}_1^0$. We have found that for produced muons of small transverse momentum corresponding to $P_t^{lim}(\mu) \approx 10GeV$ the identification remains valid for neutralino masses up to $m_{\tilde{\chi}_1^0} \approx 750GeV$ and mass differences up to $m_{\tilde{\chi}_1^\pm} - m_{\tilde{\chi}_1^0} \approx 750GeV$.

5.4 Discovery potential

In Fig.6, we present exclusion plots at the 5σ level in the plane λ_{121} versus $m_{\tilde{\nu}_\mu}$ based on the study of the $4l + \not{E}$ final state for several points of the SUSY parameter space and at a center of mass energy of $\sqrt{s} = 500GeV$ assuming a luminosity of $\mathcal{L} = 500fb^{-1}$ [45]. The considered signal and backgrounds are respectively the single $\tilde{\chi}_1^\pm$ production and the pair productions of all the neutralinos and sneutrinos. The curves of Fig.6 correspond to a number of signal events larger than 10. An efficiency of 30% has been assumed for the reconstruction of the tau-lepton from its hadronic decay. The experimental LEP limit on the sneutrino mass $m_{\tilde{\nu}} > 78GeV$ [24] has been respected. We have included the ISR effects as well as the effects of the polarization described in Section 5.1, assuming an electron (positron) polarization efficiency of 85% (60%). The cuts described in Section 5.3 have also been applied. In particular, we have applied some cuts on the transverse momentum of the produced muon. Since the value of the muon transverse momentum depends on the sneutrino and chargino masses (see Section 5.3.2), different cuts have been chosen which were appropriate to the different values of $m_{\tilde{\nu}_\mu}$ and $m_{\tilde{\chi}_1^\pm}$ considered in Fig.6.

We can observe in Fig.6 that the sensitivity on the λ_{121} coupling constant typically increases as the sneutrino mass approaches the resonance point $m_{\tilde{\nu}} = \sqrt{s} = 500GeV$. This is due to the ISR effect which increases the single chargino production rate as discussed in Section 5.2.1. While the ISR effect is significant in the domain where $m_{\tilde{\nu}_\mu} > m_{\tilde{\chi}_1^\pm} + m_{\mu^\mp}$ and $m_{\tilde{\nu}_\mu} < \sqrt{s}$, it is small for $m_{\tilde{\nu}_\mu} < m_{\tilde{\chi}_1^\pm} + m_{\mu^\mp}$ or $m_{\tilde{\nu}_\mu} > \sqrt{s}$, the reason being that in the former case the single chargino production occurs through the production of an on shell sneutrino as explained in Section 5.3.2. This results in a decrease of the sensitivity on the λ_{121} coupling at $m_{\tilde{\nu}_\mu} \gtrsim \sqrt{s}$ and $m_{\tilde{\nu}_\mu} \gtrsim m_{\tilde{\chi}_1^\pm}$ as illustrate the various curves of Fig.6. The decrease of the sensitivity corresponding to $m_{\tilde{\nu}_\mu} \gtrsim m_{\tilde{\chi}_1^\pm}$ occurs at larger sneutrino masses for the point C compared to the other SUSY points, since for this set of SUSY parameters the chargino mass is larger: $m_{\tilde{\chi}_1^\pm} = 329.9GeV$.

For $m_{\tilde{\nu}} < m_{\tilde{\chi}_1^\pm}$ the decay $\tilde{\chi}_1^\pm \to \tilde{\chi}_1^0 l_p \nu_p$ becomes dominant as explained in Section 5.2.1. This results in an increase of the sensitivity on λ_{121} which can be seen for the point C between $m_{\tilde{\nu}} \approx 330GeV$ and $m_{\tilde{\nu}} \approx 260GeV$ and for the points B and E between $m_{\tilde{\nu}} \approx 190GeV$ and $m_{\tilde{\nu}} \approx 160GeV$.

Additional comments must be made concerning the exclusion curve obtained for the point C: The decrease of sensitivity in the interval $260GeV \gtrsim m_{\tilde{\nu}} \gtrsim 200GeV$ comes from the increase of the sneutrino pair production cross section (see Section 5.2.2), while the increase of sensitivity in the range $200GeV \gtrsim m_{\tilde{\nu}} \gtrsim 160GeV$ is due to an increase of the single chargino production rate which receives in this domain

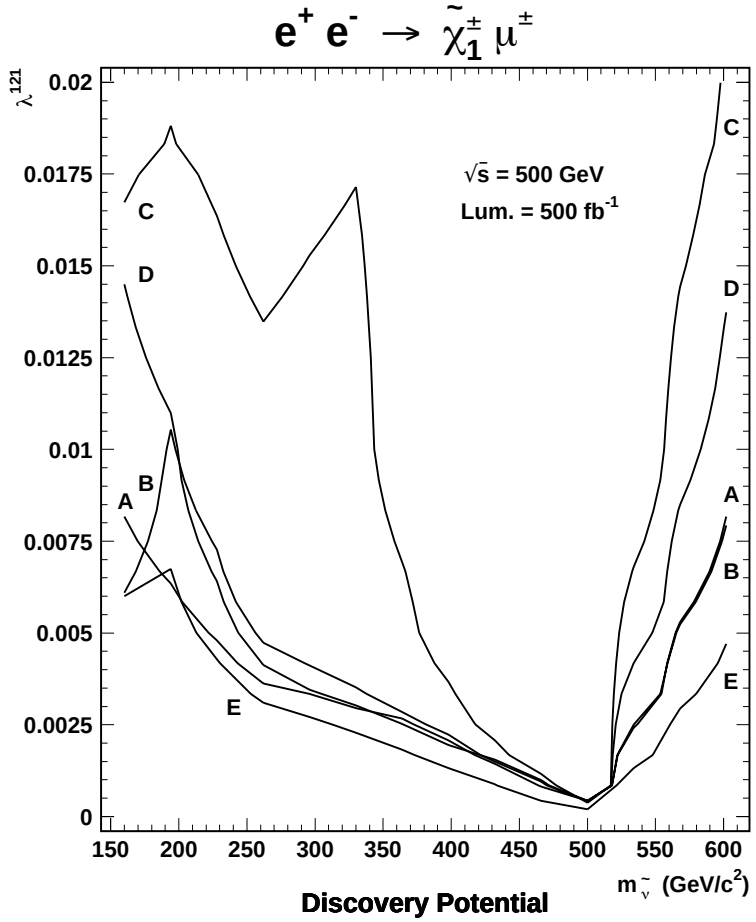

Figure 6: *Discovery potential at the 5σ level in the plane λ_{121} versus $m_{\tilde{\nu}}$ (in GeV/c^2) for the points A, B, C, D, E of the SUSY parameter space (see text) at a center of mass energy of $500GeV$ and assuming a luminosity of $\mathcal{L} = 500fb^{-1}$. The domains of the SUSY parameter space situated above the curves correspond to $S/\sqrt{B} \geq 5$ where S is the $4l + \not{E}$ signal generated by the single $\tilde{\chi}_1^{\pm}$ production and B is the R_p-conserving SUSY background.*

an important t channel contribution. The significant sensitivity on the λ_{121} coupling obtained for the point C in the interval $330GeV \gtrsim m_{\tilde{\nu}} \gtrsim 160GeV$ emphasizes the importance of the off-resonance contribution in the single chargino production study at linear colliders. For $m_{\tilde{\nu}} > 500GeV$, the sensitivity obtained with the point C is weak with respect to the other SUSY points due to the high chargino mass which suppresses the signal cross section.

We also see in Fig.6 that there are no important differences between the exclusion curves obtained for the SUSY points belonging to the higgsino region (point A), the wino region (point B) and the intermediate domain (point D). The reason is the following. The single chargino production has a cross section which decreases as going from the wino region to the higgsino region (see Section 5.2.1). However, this is also true for the $\tilde{\nu}_p \tilde{\nu}_p^*$ and most of the $\tilde{\chi}_i^0 \tilde{\chi}_j^0$ productions (see Section 5.2.2). Therefore, the sensitivities on the λ_{121} coupling obtained in the higgsino and wino region are of the same order.

Finally, we discuss the sensitivity obtained for the point E which is defined as the point B but with a smaller charged slepton mass. Although the neutralino pair production rate is larger for the point E than for the point B (see Section 5.2.2), the sensitivity obtained on λ_{121} is higher for the point E in all the considered range of sneutrino mass. This is due to the branching ratio $B(\tilde{\chi}_1^{\pm} \to \tilde{\chi}_1^0 l_p \nu_p)$ which becomes important at the point E due to the hierarchy $m_{\tilde{\chi}_1^{\pm}} > m_{\tilde{l}^{\pm}}$ (see Section 5.2.1).

We mention that the sensitivity on the λ_{121} coupling tends to decrease as $\tan\beta$ increases (for $sign(\mu) >$

0) and is weaker for $sign(\mu) < 0$ (with $\tan\beta = 3$) due to the evolution of the single chargino production rate which was described in Section 5.2.1. However, the order of magnitude of the sensitivity on λ_{121} found in Fig.6 remains correct for either large $\tan\beta$, as for instance $\tan\beta = 50$, or negative μ.

Let us make some concluding remarks. We see in Fig.6 that the sensitivity on the λ_{121} coupling reaches values typically of order 10^{-4} at the sneutrino resonance. We also observe that for each SUSY point the 5σ limit on the λ_{121} coupling remains more stringent than the low-energy limit at 2σ, namely $\lambda_{121} < 0.05\ (m_{\tilde{e}_R}/100GeV)$ [9], over an interval of the sneutrino mass of $\Delta m_{\tilde{\nu}} \approx 500GeV$ around the $\tilde{\nu}$ pole. Therefore, the sensitivities on the SUSY parameters obtained via the single chargino production analysis at linear colliders would greatly improve the results derived from the LEP analysis (see Section 1). Besides, the range of λ_{121} coupling constant values investigated at linear colliders through the single chargino production analysis (see Fig.6) would be complementary to the sensitivities obtained via the displaced vertex analysis (see Eq.(3)).

5.5 SUSY mass spectrum

5.5.1 Lightest chargino and sneutrino

First, the sneutrino mass can be determined through the study of the $4l + \not{E}$ final state by performing a scan on the center of mass energy in order to find the value of $\sqrt{s}$ at which hold the peak of the cross section associated to the sneutrino resonance. The accuracy on the measure of the sneutrino mass should be of order $\delta m_{\tilde{\nu}} \sim \sigma_{\sqrt{s}}$, where $\sigma_{\sqrt{s}}$ is the root mean square spread in center of mass energy given in terms of the beam resolution R by [48],

$$\sigma_{\sqrt{s}} = (7MeV)(\frac{R}{0.01\%})(\frac{\sqrt{s}}{100GeV}). \tag{13}$$

The values of the beam resolution at linear colliders are expected to verify $R > 1\%$.

Besides, the $\tilde{\chi}_1^{\pm}$ mass can be deduced from the transverse momentum distribution of the muon produced with the chargino. The reason is that, as we have explained in Section 5.3.2, the value of the muon transverse momentum limit $P_t^{lim}(\mu)$ is a function of the $\tilde{\chi}_1^{\pm}$ and $\tilde{\nu}$ masses. In order to discuss the experimental determination of the chargino mass, we consider separately the scenarios of negligible and significant ISR effect.

In the scenario where the ISR effect is negligible ($m_{\tilde{\nu}_\mu} < m_{\tilde{\chi}_1^{\pm}} + m_{\mu^{\mp}}$ or $m_{\tilde{\nu}_\mu} > \sqrt{s}$), the value of the muon transverse momentum limit $P_t^{lim}(\mu)$ is equal to $(E(\mu)^2 - m_{\mu^{\pm}}^2 c^4)^{1/2}/c$, $E(\mu)$ being calculated in a good approximation with Eq.(4), as described in Section 5.3.2. Since Eq.(4) gives $E(\mu)$ as a function of the center of mass energy and the chargino mass, the experimental value of $P_t^{lim}(\mu)$ would allow to determine the $\tilde{\chi}_1^{\pm}$ mass.

We now estimate the accuracy on the chargino mass measured through this method. In this method, the first source of error comes from the fact that to calculate the value of $E(\mu)$ in $P_t^{lim}(\mu) = (E(\mu)^2 - m_{\mu^{\pm}}^2 c^4)^{1/2}/c$, we use the two-body kinematics formula of Eq.(4) so that the small ISR effect is neglected. In order to include this error, we rewrite the transverse momentum kinematic limit as $P_t^{lim}(\mu) \pm \delta P_t^{lim}(\mu) = (E(\mu)^2 - m_{\mu^{\pm}}^2 c^4)^{1/2}/c$, $E(\mu)$ being calculated using Eq.(4). By comparing the value of $E(\mu)$ calculated with Eq.(4) and the value of $P_t^{lim}(\mu)$ obtained from the transverse momentum distribution, we have found that $\delta P_t^{lim}(\mu) \sim 1GeV$. One must also take into account the experimental error on the measure of the muon transverse momentum expected at linear colliders which is given by: $\delta P_t^{exp}(\mu)/P_t(\mu)^2 \leq 10^{-4}(GeV/c)^{-1}$ [45]. Hence, we take $\delta P_t^{lim}(\mu) \sim 1GeV + P_t^{lim}(\mu)^2 10^{-4}(GeV/c)^{-1}$. The experimental error on the muon transverse momentum limit depends on the value of $P_t^{lim}(\mu)$ itself and thus on the SUSY parameters and on the center of mass energy. However, we have found that in the single chargino production analysis at $\sqrt{s} = 500GeV$, the experimental error on the muon transverse momentum limit never exceeds $\sim 5GeV$. Another source of error in the measure of the $\tilde{\chi}_1^{\pm}$ mass is the root mean square spread in center of mass energy $\sigma_{\sqrt{s}}$ which is given by Eq.(13).

For instance, at the point A with $m_{\tilde{\nu}} = 550GeV$ and an energy of $\sqrt{s} = 500GeV$, the muon transverse momentum distribution, which is shown in Fig.5, gives a value for the transverse momentum limit of $P_t^{lim}(\mu) = 236.7GeV/c$. This value leads through Eq.(4) to a chargino mass of $m_{\tilde{\chi}_1^{\pm}} = 115.3 \pm 29.7GeV$ taking into account the different sources of error and assuming a beam resolution of $R = 1\%$ at linear colliders. Here, the uncertainty on the chargino mass is important due to the large value of $P_t^{lim}(\mu)$ which increases the error $\delta P_t^{lim}(\mu)$.

In the scenario where the ISR effect is important ($m_{\tilde{\nu}_\mu} > m_{\tilde{\chi}_1^\pm} + m_{\mu^\mp}$ and $m_{\tilde{\nu}_\mu} < \sqrt{s}$), the three-body kinematics of the reaction $e^+e^- \to \tilde{\chi}_1^\pm \mu^\mp \gamma$ leaves the muon energy and thus the whole muon momentum $P(\mu) = (E(\mu)^2 - m_{\mu^\pm}^2 c^4)^{1/2}/c$ unfixed by the SUSY parameters, since the muon energy depends also on the angle between the muon and the photon. Hence, $P(\mu)$ cannot bring any information on the SUSY mass spectrum. In contrast, the experimental measure of the muon transverse momentum limit $P_t^{lim}(\mu)$ would give the $\tilde{\chi}_1^\pm$ mass as a function of the $\tilde{\nu}_\mu$ mass since $P_t^{lim}(\mu) \approx (E^\star(\mu)^2 - m_{\mu^\pm}^2 c^4)^{1/2}/c$ (see Section 5.3.2) and $E^\star(\mu)$ is a function of $m_{\tilde{\chi}_1^\pm}$ and $m_{\tilde{\nu}_\mu}$ (see Eq.(12). Assuming that the $\tilde{\nu}_\mu$ mass has been deduced from the scan on the center of mass energy mentioned above, one could thus determine the $\tilde{\chi}_1^\pm$ mass.

Let us evaluate the degree of precision in the measure of $m_{\tilde{\chi}_1^\pm}$ through this calculation. First, we rewrite the transverse momentum limit as $P_t^{lim}(\mu) \pm \delta P_t^{lim}(\mu) = (E^\star(\mu)^2 - m_{\mu^\pm}^2 c^4)^{1/2}/c$ to take into account the error $\delta P_t^{lim}(\mu)$ coming from the fact that the emission angle of the radiated photon with the beam axis is neglected (see Section 5.3.2). By comparing the value of $E^\star(\mu)$ calculated with Eq.(12) and the value of $P_t^{lim}(\mu)$ obtained from the transverse momentum distribution, we have found that $\delta P_t^{lim}(\mu) \sim 1GeV$. In order to consider the experimental error on $P_t^{lim}(\mu)$, we take as before $\delta P_t^{lim}(\mu) \sim 1GeV + P_t^{lim}(\mu)^2 10^{-4}(GeV/c)^{-1}$. One must also take into account the error on the sneutrino mass. We assume that this mass has been preliminary determined up to an accuracy of $\delta m_{\tilde{\nu}} \sim \sigma_{\sqrt{s}}$.

For example, the transverse momentum distribution of Fig.3, which has been obtained for the point A with $m_{\tilde{\nu}} = 240GeV$ and $\sqrt{s} = 500GeV$, gives a value for the transverse momentum limit of $P_t^{lim}(\mu) = 92.3GeV$. The chargino mass derived from this value of $P_t^{lim}(\mu)$ via Eq.(12) is $m_{\tilde{\chi}_1^\pm} = 115.3 \pm 5.9GeV$, if the various uncertainties are considered and assuming that $\sigma_{\sqrt{s}} \sim 3.5GeV$ which corresponds to $R = 1\%$ and $\sqrt{s} = 500GeV$ (see Eq.(13)).

Hence, the $\tilde{\chi}_1^\pm$ mass can be determined from the study of the peak in the muon transverse momentum distribution in the two scenarios of negligible and significant ISR effect. The regions in the SUSY parameter space where a peak associated to the signal can be observed over the SUSY background at the 5σ level are shown in Fig.6. These domains indicate for which SUSY parameters $P_t^{lim}(\mu)$ and thus the chargino mass can be determined, if we assume that as soon as a peak is observed in the muon transverse momentum distribution the upper kinematic limit of this peak $P_t^{lim}(\mu)$ can be measured.

5.5.2 Heaviest chargino

The single $\tilde{\chi}_2^\pm$ production $e^+e^- \to \tilde{\chi}_2^\pm \mu^\mp$ is also of interest at linear colliders. This reaction, when kinematically open, has a smaller phase space factor than the single $\tilde{\chi}_1^\pm$ production. Hence, the best sensitivity on the λ_{121} coupling is obtained from the study of the single $\tilde{\chi}_1^\pm$ production. However, for sufficiently large values of the λ_{121} coupling, the $e^+e^- \to \tilde{\chi}_2^\pm \mu^\mp$ reaction would allow to determine either the $\tilde{\chi}_2^\pm$ mass or a relation between the $\tilde{\chi}_2^\pm$ and $\tilde{\nu}$ masses. As described in Section 5.5.1, those informations could be derived from the upper kinematic limit $P_t^{lim}(\mu)$ of the peak associated to the single $\tilde{\chi}_2^\pm$ production observed in the muon transverse momentum distribution. Indeed, the method presented in the study of the single $\tilde{\chi}_1^\pm$ production remains valid for the single $\tilde{\chi}_2^\pm$ production analysis.

The simultaneous determination of the $\tilde{\chi}_1^\pm$ and $\tilde{\chi}_2^\pm$ masses is possible since the peaks in the muon transverse momentum distribution corresponding to the single $\tilde{\chi}_1^\pm$ and $\tilde{\chi}_2^\pm$ productions can be distinguished and identified. In order to discuss this point, we present in Fig.7 the muon transverse momentum distribution for the $4l + \not{E}$ events generated by the reactions $e^+e^- \to \tilde{\chi}_1^\pm \mu^\mp$ and $e^+e^- \to \tilde{\chi}_2^\pm \mu^\mp$ and by the SUSY background at the MSSM point A (for which $m_{\tilde{\chi}_1^\pm} = 115.7GeV$ and $m_{\tilde{\chi}_2^\pm} = 290.6GeV$) with $\lambda_{121} = 0.05$ and $m_{\tilde{\nu}} = 450GeV$. The cuts described in Section 5.3.1 have not been applied. In this Figure, we observe that the peak associated to the single $\tilde{\chi}_2^\pm$ production appears at smaller values of the transverse momentum than the peak caused by the single $\tilde{\chi}_1^\pm$ production. This is due to the hierarchy of the chargino masses. Indeed, the chargino masses enter the formula of Eq.(12) which gives the values of $P_t^{lim}(\mu) \approx (E^\star(\mu)^2 - m_{\mu^\pm}^2 c^4)^{1/2}/c$ for the point A with $m_{\tilde{\nu}} = 450GeV$. The same difference between the two peaks is observed in the scenario where the values of $P_t^{lim}(\mu) \approx (E(\mu)^2 - m_{\mu^\pm}^2 c^4)^{1/2}/c$ are calculated using the formula of Eq.(4), namely for $m_{\tilde{\nu}_\mu} < m_{\tilde{\chi}_1^\pm} + m_{\mu^\mp}$ and $m_{\tilde{\nu}_\mu} < m_{\tilde{\chi}_2^\pm} + m_{\mu^\mp}$, or $m_{\tilde{\nu}_\mu} > \sqrt{s}$. Fig.7 also illustrates the fact that the peaks associated to the single $\tilde{\chi}_1^\pm$ and $\tilde{\chi}_2^\pm$ productions can be easily identified thanks to their relative heights. The difference between the heights of the two peaks is due to the relative values of the cross sections and branching ratios which read for instance with the SUSY

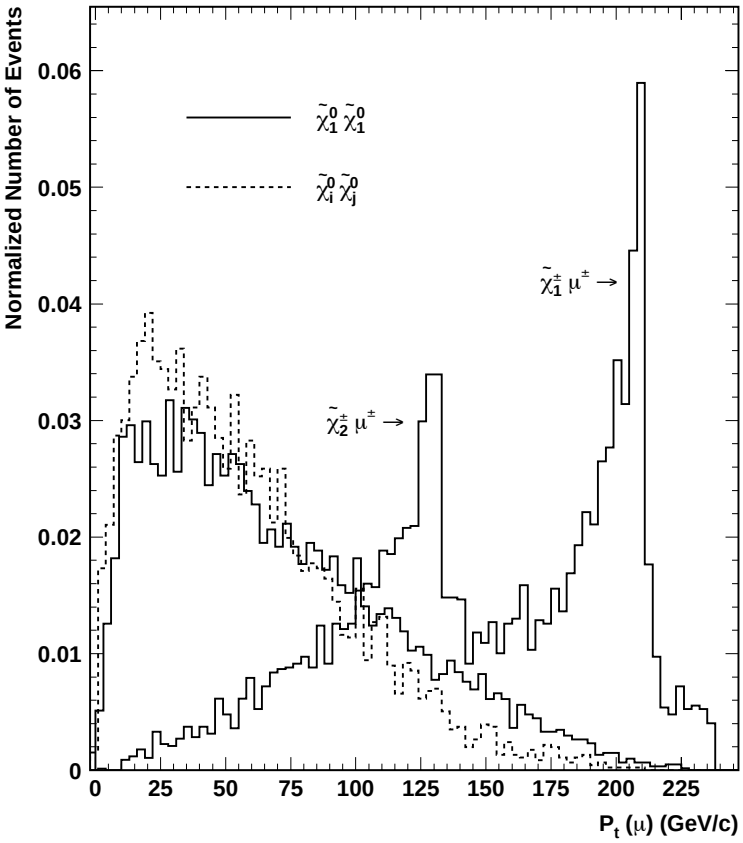

Figure 7: *Distributions of the highest muon transverse momentum $P_t(\mu)$ (in GeV/c) for the $4l+\not{E}$ events generated by the single chargino productions ($\tilde{\chi}_1^\pm + \tilde{\chi}_2^\pm$) and the SUSY background which is divided into the $\tilde{\chi}_1^0\tilde{\chi}_1^0$ and $\tilde{\chi}_i^0\tilde{\chi}_j^0$ productions. The number of events for each distribution is normalized to the unity, the center of mass energy is fixed at $500GeV$ and the point A of the SUSY parameter space is considered with $\lambda_{121} = 0.05$ and $m_{\tilde{\nu}} = 450GeV$.*

parameters of Fig.7 as (including the beam polarization described in Section 5.1): $\sigma(\tilde{\chi}_1^\pm\mu^\mp) = 620.09fb$, $\sigma(\tilde{\chi}_2^\pm\mu^\mp) = 605.48fb$, $B(\tilde{\chi}_1^\pm \to \tilde{\chi}_1^0 l^\pm \not{E}) = 33.9\%$ and $B(\tilde{\chi}_2^\pm \to \tilde{\chi}_1^0 l^\pm \not{E}) = 10.8\%$.

5.6 Extension of the analysis to different center of mass energies

In this section, we comment on a similar study of the reaction $e^+e^- \to \tilde{\chi}^\pm\mu^\mp$ based on the $4l + \not{E}$ events at center of mass energies different from $\sqrt{s} = 500GeV$.

First, the muon transverse momentum distributions depend mainly on the relative values of the center of mass energy and of the various SUSY masses, so that the discussion on the cuts given in Section 5.3 still hold for different energies. The reconstruction of the $\tilde{\chi}_{1,2}^\pm$ and $\tilde{\nu}$ masses through the methods exposed in Section 5.5 is possible at any center of mass energy. We thus discuss in this section the sensitivity on the λ_{121} coupling that would be obtained at other center of mass energies than $\sqrt{s} = 500GeV$.

Similarly, the values of the branching ratios are function of the SUSY mass spectrum, as shown in Sections 5.2.1 and 5.2.2, and thus do not change if the center of mass energy is modified.

Besides, the amplitude of the ISR effect on the signal cross section depends on the relative values of $m_{\tilde{\nu}}$, $m_{\tilde{\chi}_1^\pm}$ and $\sqrt{s}$ (see Section 5.3.2). The shapes of the exclusion curves obtained at different center of mass energies would thus be similar to the shapes of the exclusion plots presented in Fig.6 for same

relative values of $m_{\tilde{\nu}}$, $m_{\tilde{\chi}_1^\pm}$ and $\sqrt{s}$.

However, the cross sections of the SUSY backgrounds, namely the $\tilde{\nu}_p\tilde{\nu}_p^*$ and $\tilde{\chi}_i^0\tilde{\chi}_j^0$ productions, depend strongly on the center of mass energy which determines the phase space factors of the superpartners pair productions.

Therefore, the sensitivity on the λ_{121} coupling tends to decrease (increase) at higher (smaller) center of mass energies due to the increase (decrease) of the SUSY background rates.

5.7 Study based on the $3l + 2jets + \not{E}$ final state

In this Section, we would like to emphasize the interest of the $3l + 2jets + \not{E}$ final state for the study of the reaction $e^+e^- \to \tilde{\chi}^\pm\mu^\mp$ at linear colliders.

First, the $3l + 2jets + \not{E}$ final state is generated by the decay $\tilde{\chi}^\pm \to \tilde{\chi}_1^0 d_p u_{p'}$ which has a larger branching ratio than the decay $\tilde{\chi}^\pm \to \tilde{\chi}_1^0 l_p \nu_p$ for the hierarchy $m_{\tilde{\nu}}, m_{\tilde{l}^\pm}, m_{\tilde{q}} > m_{\tilde{\chi}_1^\pm}$, as mentioned in Section 5.2.1.

Secondly, the Standard Model background of the $3l + 2jets + \not{E}$ signature is the WWZ production. The rate of the $3l + 2jets + \not{E}$ production from the $e^+e^- \to WWZ$ reaction is $1.5fb$ ($0.5fb$) at $\sqrt{s} = 500GeV$ ($350GeV$) including the cuts $|\eta(l)| < 3$, $P_t(l) > 10GeV$ and neglecting the ISR [2]. This background can be further reduced as explained in Section 4.2. Besides, the $3l + 2jets + \not{E}$ signature has no R_p-conserving SUSY background if one assumes that the LSP is the $\tilde{\chi}_1^0$ and that the single dominant $\not{R}_p$ coupling is λ_{121}. Indeed, the pair productions of SUSY particles typically lead to final states wich contain at least 4 charged leptons due to the decay of the two LSP's through λ_{121} as $\tilde{\chi}_1^0 \to l\bar{l}\nu$.

Therefore, the sensitivity on the λ_{121} coupling obtained from the study of the single chargino production based on the $3l + 2jets + \not{E}$ final state should be greatly enhanced with respect to the analysis of the $4l + \not{E}$ signature.

The $3l + 2jets + \not{E}$ final state is also attractive from the mass reconstruction point of view. Indeed, the full decay chain $\tilde{\chi}_1^\pm \to \tilde{\chi}_1^0 d_p u_{p'}$, $\tilde{\chi}_1^0 \to l\bar{l}\nu$ can be reconstructed. The reason is that, since the muon produced together with the chargino in the reaction $e^+e^- \to \tilde{\chi}_1^\pm\mu^\mp$ can be identified (see Section 5.3.2) the origin of each particle in the final state can be known. First, the $\tilde{\chi}_1^0$ mass can be measured with the distribution of the invariant mass of the two charged leptons coming from the $\tilde{\chi}_1^0$ decay: The value of the $\tilde{\chi}_1^0$ mass is readen at the upper endpoint of this distribution. Similarly, the upper endpoint of the invariant mass distribution of the two jets coming from the chargino decay gives the mass difference $m_{\tilde{\chi}_1^\pm} - m_{\tilde{\chi}_1^0}$. Since $m_{\tilde{\chi}_1^0}$ has already been determined from the dilepton invariant mass, we can deduce from this mass diffference the $\tilde{\chi}_1^\pm$ mass.

Besides, the $\tilde{\nu}$ and $\tilde{\chi}_{1,2}^\pm$ masses can be measured as explained in Section 5.5.

Hence, in the case of a non-vanishing λ coupling with $\tilde{\chi}_1^0$ as the LSP, the combinatorial background for the $\tilde{\chi}_1^0$ mass reconstruction from the study of the single chargino production based on the $3l + 2jets + \not{E}$ final state is expected to be greatly reduced with respect to the analysis based on the pair production of SUSY particles [7], due to the better identification of the charged leptons coming from the $\tilde{\chi}_1^0$ decay. Furthermore, while the $\tilde{\chi}_{1,2}^\pm$ and $\tilde{\nu}$ masses reconstructions are possible via the single chargino production, these reconstructions appear to be more difficult with the pair production of SUSY particles. Indeed, the $\tilde{\chi}^\pm$ and $\tilde{\nu}$ masses reconstructions from the superpartner pair production are based on the $\tilde{\chi}_1^0$ reconstruction, and moreover in the pair prodution the $\tilde{\chi}^\pm$ or $\tilde{\nu}$ decays lead to either an additional uncontroled missing energy or an higher number of charged particles (or both) in the final state with respect to the single chargino production signature.

5.8 Study of the single chargino production through various $\not{R}_p$ couplings

The single chargino production at muon colliders $\mu^+\mu^- \to \tilde{\chi}^\pm l_m^\mp$ (see Fig.1) would allow to study the λ_{2m2} coupling, m being equal to either 1 or 3 due to the antisymmetry of the λ_{ijk} couplings.

The study of the λ_{212} coupling would be essentially identical to the study of λ_{121}. Only small modifications would enter the analysis: Since an electron/positron would be produced together with the chargino, one should require that the final state contains at least one electron instead of one muon as in the λ_{121} case (Section 5.3.1). Besides, one should study the distribution of the highest electron transverse momentum instead of the highest muon transverse momentum. The particularities of the muon colliders would cause other differences in the study: First, the analysis would suffer an additional background due to the μ decays in the detector. Secondly, large polarization would imply sacrifice in luminosity since

at muon colliders this is achieved by keeping only the larger p_z muons emerging from the target [49]. Therefore, one expects an interesting sensitivity on the λ_{212} coupling from the single $\tilde{\chi}_1^\pm$ production at muon colliders although this sensitivity should not be as high as in the study of the λ_{121} coupling at linear colliders.
Besides, the $\mu^+\mu^- \to \tilde{\chi}^\pm e^\mp$ reaction occuring through λ_{212} would allow to determine the $\tilde{\chi}_1^0$, $\tilde{\chi}_1^\pm$, $\tilde{\chi}_2^\pm$ and $\tilde{\nu}$ masses as described in Sections 5.5 and 5.7 for the single chargino production at linear colliders. The main difference would be the following. The accuracy in the determination of the sneutrino mass performed through a scan over the center of mass energy would be higher at muon colliders than at linear colliders. The reason is the high beam resolution R expected at muon colliders (see Section 5.5.1). For instance, at muon colliders the beam resolution should reach $R \sim 0.14\%$ for a luminosity of $\mathcal{L} = 10 fb^{-1}$ and an energy of $\sqrt{s} = 300 - 500 GeV$ [49].

The production of a single chargino together with a tau-lepton occurs through the λ_{131} coupling at linear colliders and via λ_{232} at muon coliders. Due to the τ-decay, the transverse momentum distribution of the produced τ-lepton cannot be obtained with a good accuracy. The strong cut on the transverse momentum described in Section 5.3.2 is thus difficult to apply in that case, and one must think of other discrimination variables such as the total transverse momentum of the event, the total missing energy, the rapidity, the polar angle, the isolation angle, the acoplanarity, the acollinearity or the event sphericity. Therefore, the sensitivities on the λ_{131} and λ_{232} couplings obtained from the $\tilde{\chi}^\pm\tau^\mp$ production should be weaker than the sensitivities expected for λ_{121} and λ_{212} respectively. Furthermore, the lack of precision in the τ transverse momentum distribution renders the reconstructions of the $\tilde{\chi}_1^0$, $\tilde{\chi}_1^\pm$ and $\tilde{\chi}_2^\pm$ masses from the $\tilde{\chi}^\pm\tau^\mp$ production (see Sections 5.5 and 5.7) difficult.

5.9 Single neutralino production

We have seen in Sections 5.3.2 and 5.4 that when the sneutrino mass is smaller than the lightest chargino mass (case of small ISR effect), the single chargino production cross section is greatly reduced at linear colliders. The reason is that in this situation the radiative return to the sneutrino resonance allowed by the ISR is not possible anymore. The interesting point is that for $m_{\tilde{\chi}_1^0} < m_{\tilde{\nu}} < m_{\tilde{\chi}_1^\pm}$, the radiative return to the sneutrino resonance remains possible in the single $\tilde{\chi}_1^0$ production through λ_{1m1}: $e^+e^- \to \tilde{\chi}_1^0\nu_m$. Therefore, in the region $m_{\tilde{\chi}_1^0} < m_{\tilde{\nu}} < m_{\tilde{\chi}_1^\pm}$ the single $\tilde{\chi}_1^0$ production has a larger rate than the single $\tilde{\chi}_1^\pm$ production and is thus attractive to test the λ_{1m1} couplings.
We give now some qualitative comments on the backgrounds of the single neutralino production. If we assume that the $\tilde{\chi}_1^0$ is the LSP, the $\tilde{\chi}_1^0\nu_m$ production leads to the $2l + \not{E}$ final state due to the $\not{R}_p$ decay $\tilde{\chi}_1^0 \to l\bar{l}\nu$. This signature is free of R_p-conserving SUSY background since the pair production of SUSY particles produces at least 4 charged leptons due to the presence of the LSP at the end of each of the 2 cascade decays. The Standard Model background is strong as it comes from the WW and ZZ productions but it can be reduced by some kinematic cuts.
Therefore, in the region $m_{\tilde{\chi}_1^0} < m_{\tilde{\nu}} < m_{\tilde{\chi}_1^\pm}$, one expects an interesting sensitivity on λ_{1m1} from the single neutralino production study which was for instance considered in [26] for muon colliders.

The single $\tilde{\chi}_1^0$ production allows also to reconstruct the $\tilde{\chi}_1^0$ mass. Indeed, the neutralino mass is given by the endpoint of the distribution of the 2 leptons invariant mass in the $2l + \not{E}$ final state generated by the single $\tilde{\chi}_1^0$ production. The combinatorial background is extremely weak since the considered final state contains only 2 charged leptons.

If the sneutrino is the LSP, when it is produced at the resonance through λ_{1m1} as $e^+e^- \to \tilde{\nu}_m$, it can only decay as $\tilde{\nu}_m \to e^+e^-$ assuming a single dominant $\not{R}_p$ coupling constant. Hence, in this scenario, the sneutrino resonance must be studied trhough its effect on the Bhabha scattering [14, 15, 18, 19]. This conclusion also holds in the case of nearly degenerate $\tilde{\nu}$ and $\tilde{\chi}_1^0$ masses since then the decay $\tilde{\nu}_m \to e^+e^-$ is dominant compared to the decay $\tilde{\nu}_m \to \tilde{\chi}_1^0\nu_m$.

6 Conclusion

The study at linear colliders of the single chargino production via the single dominant λ_{121} coupling $e^+e^- \to \tilde{\chi}^\pm\mu^\mp$ is promising, due to the high luminosities and energies expected at these colliders. Assuming that the $\tilde{\chi}_1^0$ is the LSP, the singly produced chargino has 2 main decay channels: $\tilde{\chi}^\pm \to \tilde{\chi}_1^0 l^\pm\nu$ and $\tilde{\chi}^\pm \to \tilde{\chi}_1^0 ud$.

The leptonic decay of the produced chargino $\tilde{\chi}^{\pm} \to \tilde{\chi}_1^0 l^{\pm} \nu$ (through, virtual or real, sleptons and W-boson) leads to the clean $4l + \not{E}$ final state which is almost free of Standard Model background. This signature suffers a large SUSY background in some regions of the MSSM parameter space but this SUSY background can be controled using the initial beam polarization and some cuts based on the specific kinematics of the single chargino production. Therefore, considering a luminosity of $\mathcal{L} = 500 fb^{-1}$ at $\sqrt{s} = 500 GeV$ and assuming the largest SUSY background, values of the λ_{121} coupling smaller than the present low-energy bound could be probed over a range of the sneutrino mass of $\Delta m_{\tilde{\nu}} \approx 500 GeV$ around the sneutrino resonance and at the $\tilde{\nu}$ pole the sensitivity on λ_{121} could reach values of order 10^{-4}. Besides, the $4l + \not{E}$ channel could allow to reconstruct the $\tilde{\chi}_1^{\pm}$, $\tilde{\chi}_2^{\pm}$ and $\tilde{\nu}$ masses.

The hadronic decay of the produced chargino $\tilde{\chi}^{\pm} \to \tilde{\chi}_1^0 ud$ (through, virtual or real, squarks and W-boson) gives rise to the $3l + 2j + \not{E}$ final state. This signature, free from SUSY background, has a small Standard Model background and should thus also give a good sensitivity on the λ_{121} coupling constant. This hadronic channel should allow to reconstruct the $\tilde{\chi}_1^0$, $\tilde{\chi}_1^{\pm}$, $\tilde{\chi}_2^{\pm}$ and $\tilde{\nu}$ masses.

The sensitivity on the λ_{131} coupling constant, obtained from the $\tilde{\chi}^{\pm}\tau^{\mp}$ production study, is expected to be weaker than the sensitivity found on λ_{121} due to the decays of the tau-lepton.

7 Acknowledgments

The author is grateful to M. Chemtob, H. U. Martyn and Y. Sirois for helpful discussions and having encouraged this work. It is also a pleasure to thank N. Ghodbane and M. Boonekamp for instructive conversations.

References

[1] H. Dreiner, published in *Perspectives on Supersymmetry*, ed. by G.L. Kane, World Scientific (1998), hep-ph/9707435.

[2] D. K. Ghosh, R. M. Godbole, S. Raychaudhuri, hep-ph/9904233.

[3] V. Barger et al., Phys. Rev. **D50**, 4299 (1994).

[4] H. Baer, C. Kao and X. Tata, Phys. Rev. **D51**, 2180 (1995).

[5] H. Baer, C.-H. Chen and X. Tata, Phys. Rev. **D55**, 1466 (1997).

[6] B. Allanach et al., 'Searching for R-Parity Violation at Run-II of the Tevatron', hep-ph/9906224.

[7] ATLAS Coll., 'ATLAS Detector and Physics Performance Technical Design Report', Vol. II, ATLAS TDR 15, 25 May 1999, CERN/LHCC 99-15, atlasinfo.cern.ch/Atlas/GROUPS/PHYSICS/TDR/-access.html.

[8] H. Dreiner and G. G. Ross, Nucl. Phys. **B 365**, 597 (1991).

[9] G. Bhattacharyya, Invited talk presented at 'Beyond the Desert', Castle Ringberg, Tegernsee, Germany, 8-14 June 1997; Susy '96, Nucl. Phys. B (Proc. Suppl.) **52A** 83 (1997).

[10] R. Barbier et al., Report of the Group on the R-parity Violation, hep-ph/9810232.

[11] S. Dimopoulos and L.J. Hall, Phys. Lett. **B 207**, 210 (1988).

[12] V. Barger, G. F. Giudice and T. Han, Phys. Rev. **D 40**, 2987 (1989).

[13] D. Choudhury, Phys. Lett. **B 376**, 201 (1996).

[14] J. Kalinowski, R. Rückl, H. Spiesberger and P. M. Zerwas, Z. Phys. **C 74**, 595 (1997).

[15] J. Kalinowski, R. Rückl, H. Spiesberger and P. M. Zerwas, Phys. Lett. **B406**, 314 (1997).

[16] J. Kalinowski, Talk presented at the 5th International Workshop on *"Deep Inelastic Scattering and QCD"* (DIS'97), Chicago, Illinois, USA, April 14-18, 1997, hep-ph/9706203.

[17] J. Kalinowski, R. Rückl, H. Spiesberger and P. M. Zerwas, Phys. Lett. **B414**, 297 (1997).

[18] J. Kalinowski, Proceedings of *"Beyond the Desert 97 – Accelerator and Non-Accelerator Approaches"*, Ringberg Castle, Germany, June 1997, hep-ph/9708490.

[19] J. Kalinowski, Acta Phys. Polon. **B28**, 2423 (1997).

[20] ALEPH Collaboration, submitted to ICHEP'98 (Abstract Number 949), ALEPH 98-070, CONF 039 (1998).

[21] Y. Arnoud et al., DELPHI Collaboration, submitted to HEP'97 (Abstract Number 589), DELPHI 97-119, CONF 101 (1997).

[22] F. Ledroit-Guillon and R. López-Fernández, DELPHI Collaboration, DELPHI 98-165, PHYS 805.

[23] F. Ledroit-Guillon and R. López-Fernández, DELPHI Collaboration, DELPHI 99-30, CONF 229 (1999).

[24] N. Benekos et al., DELPHI Collaboration, submitted to HEP'99 (Abstract Number 7_209), DELPHI 99-79, CONF 266 (1999).

[25] J. Erler, J. L. Feng and N. Polonsky, Phys. Rev. Lett. **78**, 3063 (1997).

[26] J. L. Feng, J. F. Gunion and T. Han, Phys. Rev. **D58**, 071701 (1998); J. L. Feng, Proceedings of the Workshop on Physics at the First Muon Collider and at the Front End of a Muon Collider, Fermi National Accelerator Laboratory, 6-9 november 1997, hep-ph/9801248.

[27] S. Bar-Shalom, G. Eilam and A. Soni, Phys. Rev. Lett. **80**, 4629 (1998).

[28] D. Choudhury and S. Raychaudhuri, hep-ph/9807373.

[29] S. Dimopoulos, R. Esmailzadeh, L.J. Hall, J. Merlo and G.D. Starkman, Phys. Rev. **D41**, 2099 (1990).

[30] P. Binétruy et al., ECFA Large Hadron Collider (LHC) Workshop, Aachen, 1990, Vol. II.

[31] D. K. Ghosh, S. Raychaudhuri and K. Sridhar, Phys. Lett. **B396**, 177 (1997).

[32] A. Datta, J. M. Yang, B.-L. Young and X. Zhang, Phys. Rev. **D56**, 3107 (1997).

[33] R. J. Oakes, K. Whisnant, J. M. Yang, B.-L. Young and X. Zhang, Phys. Rev. **D57**, 534 (1998).

[34] S. Bar-Shalom, G. Eilam and A. Soni, Phys. Rev. **D59**, 055012 (1999).

[35] J. L. Hewett and T. G. Rizzo, "Proceedings of the XXIX International Conference on High Energy Physics", Vancouver, CA, 23-29 July 1998, hep-ph/9809525.

[36] H. Dreiner, P. Richardson and M. H. Seymour, to appear in the proceedings of the BTMSSM subgroup of the Physics at Run II Workshop on Supersymmetry/Higgs, hep-ph/9903419.

[37] E. L. Berger, B. W. Harris and Z. Sullivan, Phys. Rev. Lett. **83**, 4472 (1999).

[38] F. Déliot, G. Moreau, C. Royon, E. Perez and M. Chemtob, Phys. Lett. **B475**, 184 (2000).

[39] H. Dreiner, P. Richardson and M. H. Seymour, hep-ph/0001224.

[40] G. Moreau, E. Perez and G. Polesello, Proceedings of the Workshop *'Physics at TeV Colliders'*, 8-18 June, 1999, Les Houches, France, hep-ph/0002130.

[41] G. Moreau, E. Perez and G. Polesello, hep-ph/0003012.

[42] H. Dreiner and S. Lola, published in " Munich-Annecy-Hamburg 1991/93, Proceedings, e^+e^- Collisions at 500 GeV: The Physics Potential ", DESY 92-123A+B, 93-123C; " Annecy-Gran Sasso-Hamburg 1995, Proceedings, e^+e^- Collisions at TeV Energies: The Physics Potential ", DESY 96-123D, ed. P. M. Zerwas; " Searches for New Physics ", contribution to the LEPII Workshop, 1996, hep-ph/9602207; " Physics with e^+e^- Linear Colliders ", DESY-97-100, hep-ph/9705442.

[43] S. Lola, Presented at the 2nd ECFA/DESY study on Linear Colliders, Frascati, November 1998, LC note LC-TH-1999-021, hep-ph/9912217.

[44] M. Chemtob and G. Moreau, Phys. Rev. **D 59**, 055003 (1999).

[45] 'Conceptual Design Report of a $500GeV$ e^+e^- Linear Collider with Integrated X-ray Laser Facility', DESY 1997-048, ECFA 1997-182, Editors: R. Brinkmann, G. Materlik, J. Rossbach and A. Wagner, www.desy.de/∼schreibr/cdr/cdr.html.
See also wwwhephy.oeaw.ac.at/susy/lcws/tdr.html.

[46] J. A. Bagger, Nucl. Phys. (Proc. Suppl.) **B 62**, 23 (1998).

[47] SUSYGEN 3.0/06, 'A Monte Carlo Event generator for MSSM sparticle production for e^+e^-, $\mu^+\mu^-$ and ep colliders', N. Ghodbane, S. Katsanevas, P. Morawitz and E. Perez, lyoinfo.in2p3.fr/susygen-/susygen3.html; N. Ghodbane, hep-ph/9909499.

[48] V. Barger, 'Physics at Muon Colliders', Talk present at FCP97, Workshop on Fundamental Particles and Interactions, Vanderbilt University, May 1997, hep-ph/9801441.

[49] J. F. Gunion, 'Muon Colliders: The Machine and The Physics', Proceedings of *"Beyond the Standard Model V"*, Balholm, Norway, May, 1997, hep-ph/9707379.